

Supporting Information

for

Py-Azo-decorated covalent organic frameworks as a structure-responsive mass spectrometry probe for high-sensitivity and high-throughput screening of trace toxic chemicals in complex samples

Li Huang,[†] Qian Wang,[†] Qiu-Rong He, Xiu Huang*, Zun-Zhen Zhang

West China School of Public Health and West China Fourth Hospital, Sichuan University, Sichuan 610041, China

[†] These authors contributed equally to this article

Corresponding author: Dr. Xiu Huang. No.16, Section 3, Renmin South Road, Chengdu 610041, China. Email: huangxiu9168@163.com (X. Huang).

Contents

1. Experimental section
2. Supplementary Tables
3. Supplementary Figures

1. Experimental section

Chemicals and Materials.

Py-Azo-COF and graphene were purchased from XFNANO (Nanjing, China). Cetyltrimethylammonium bromide (CTAB) and bovine serum albumin V (BSA-V) were obtained from Solarbio (Beijing, China). Humic acid (HA), perfluorononanoic acid (PFOA), α -cyano-4-hydroxycinnamic acid (CHCA), n-hexane and acetonitrile were sourced from Macklin (Shanghai, China). Bisphenol A (BPA), 4,4'-sulfonyldiphenol (BPS), 2-hydroxy-4-methoxybenzophenone (BP-3), heneicosafuoroundecanoic acid (PFUNA), myristyltrimethylammonium bromide (TTAB), benzyldimethyltetradecylammonium chloride hydrate (TDBAC), 3,3,5,5-tetrabromobisphenol A (TBBPA), perfluorodecanoic acid (PFDA), nonafluorobutane-1-sulfonic acid (PFBS) and alkyl-benzyl-dimethylammonium chloride (BAC) were purchased from Aladdin (Shanghai, China). Methanol, ethanol and sodium chloride (NaCl) were provided by Keshi (Chengdu, China). Standard buffer solution (pH 4 and pH 10) was purchased from Senhope Standard Technology Co. (Xiamen, China). Ultrapure water was prepared using a Merck Milli-Q system (Darmstadt, Germany). All chemicals used were analytical grade unless otherwise specified.

Characterization of Py-Azo-COF.

TEM images were captured by Thermo Fisher Scientific Spectra300 Hitachi S-3000N transmission electron microscope with double spherical aberration correction (Massachusetts, USA). BET was acquired by Micromeritics TriStar II Plus Brunauer-Emmet-Teller (Georgia, USA). XRD pattern was obtained using a Malvern Panalytical Empyrean X-ray diffractometer (Almelo, Netherlands). NMR spectra was acquired by Bruker Avance II-400 MHz nuclear magnetic resonance spectrometer (Massachusetts, USA). FTIR spectra was obtained using Attenuated Total Reflection (ATR) on a Thermo Nicolet NEXUS 670 Fourier transform infrared spectrometer (Wisconsin, USA). XPS spectra were acquired using a Kratos AXIS Supra X-ray Photoelectron Spectrometer (Manchester, UK) with Al K α X-ray radiation as the excitation source.

UV-visible spectra were obtained using a Shimadzu UV2700i UV-visible spectrophotometer (Kyoto, Japan).

MALDI-TOF MS.

The experiments were carried out using a Shimadzu Axima Performance MALDI-TOF mass spectrometer (Kyoto, Japan), which was equipped with a 337 nm nitrogen laser. The laser operated at a frequency of 85 Hz, with power adjusted to a threshold level to achieve a high-intensity signal while minimizing noise in the mass spectra. The sample mixture solution was prepared by mixing twelve toxic chemical standards in equal proportions. Py-Azo-COF was dispersed in ultrapure water at a concentration of 1 mg/mL with the aid of ultrasound to obtain a matrix dispersion. The sample mixture solution and matrix dispersion were then mixed in a 1:1 (v/v) ratio. Subsequently, 1.5 μ L of the mixture was dropped onto the MALDI target plate. The plate was then allowed to desiccate under ambient conditions before MALDI-TOF MS analysis.

Each sample consists of three parallel samples, with two sample points on the MALDI target plate for each of them. The mass spectra were obtained by summing 100 laser shots using an 85 Hz laser pulse power. Each spectrum was recorded by performing 10 shots in different sample regions, and the spectrum with average intensities was selected to ensure its representativeness. The peak intensity was determined while considering the molecular ion peaks with the signal-to-noise ratio (S/N) greater than 3. The target compounds were subjected to mass spectrometry analysis in both positive and negative ionization modes. Data were processed using the Shimadzu Biotech MALDI-TOF MS software.

SALDI-TOF MS.

The Py-Azo-COF probe was dispersed in ultrapure water with the aid of ultrasound, resulting in a concentration of 1 mg/mL. Twelve toxic chemical standards were mixed in equal proportions to form the standard sample mixture solution. To test the dispersibility and stability of Py-Azo-COF in different solvents, the dispersion was prepared using methanol, ethanol, n-hexane and water as solvents. Subsequently, 600 μ L of the probe was added into 600 μ L sample and 300 μ L of solvents using vibration

for 30 minutes to enrich the target analytes. To assess the influence of environmental and biological factors on the SALDI probe, separate solutions of HA, NaCl, and BSA were added to a solution containing 600 μL of the probe and 600 μL sample. The probes were then incubated at room temperature for 24 hours, collected and centrifuged at 1500 rpm for 10 minutes. The resulting supernatant was discarded and 10 μL precipitate was obtained. The precipitate (1.5 μL) was subsequently deposited on the MALDI target for analysis.

Molecular docking.

The 3D structure of Py-Azo-COF was generated using Chem 3D. The receptor and ligand structures of Py-Azo-COF were optimized individually with xTB software at the GFN2-xTB level, incorporating the ALPB implicit solvation model to simulate aqueous environments. Binding poses were predicted using Autodock Vina's docking submodule. This submodule employs an automated Interaction Site Screening (aISS) protocol, which screens potential interaction sites and conducts genetic optimization based on xTB-IFF energy, followed by geometry optimizations at the GFN level.

Analysis of Environment Samples.

The wastewater samples ($n = 12$) and sewage sludge samples ($n = 12$) were collected from various electronic factories in Chengdu. The collected sewage sludge samples were subjected to pressure steam sterilization treatment. The sewage sludge samples were then dissolved in ultrapure water and sonicated for 30 minutes. After being leached in ultrapure water for 24 hours, the mixture was centrifuged at 1500 rpm for 10 minutes and the resulting supernatant was used for analysis. Subsequently, 300 μL of probe was added with 100 μL of the supernatant and 100 μL of ultrapure water by vibration for 30 minutes to enrich the target analytes. Following the incubation at room temperature for 24 hours, the probe was collected and centrifuged at 1500 rpm for 10 minutes. The supernatant was then discarded and the resulting precipitate (1.5 μL) was deposited on the MALDI target for MALDI-TOF MS analysis.

HPLC-ESI-MS.

To validate the results obtained from SALDI-TOF MS, the concentrations of target chemicals in both wastewater and sewage sludge samples were determined using a liquid chromatography mass spectrometry system (LC-MS, AB SCIEX QTRAP 4500). The sample pretreatment procedures closely followed those reported previously to ensure consistency. To minimize potential analyte loss, a straightforward pretreatment procedure was employed. A sewage sludge sample weighing approximately 1.0 g was mixed with 10 mL of ultrapure water in a 15 mL centrifuge tube. The mixture underwent sonication at 40 °C for 45 minutes and subsequent centrifugation at 10000 rpm for 5 minutes. The wastewater samples were centrifuged at 10000 rpm for 5 minutes, and the resulting supernatant was transferred to another tube. This extraction process was repeated three times.

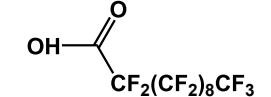
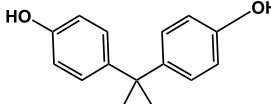
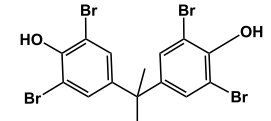
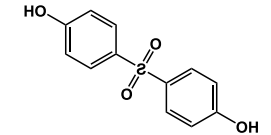
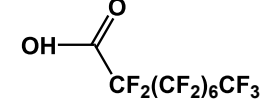
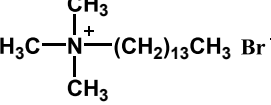
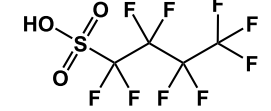
The identification and quantification procedures were conducted using an LC-MS (AB SCIEX, Framingham, MA) system in full scan mode (m/z 50–800) with a resolution of 60000. Electrospray ionization was employed in multiple response monitoring scan mode, with the ion spray voltage set at 4500 V, temperature at 450 °C, ion source gas at 30 psi, and curtain gas at 9 psi. Analyte separation was accomplished by utilizing a Phenomenex Kinetex C18 column (2.1 mm inner diameter \times 100 mm length, 2.6 μ m, Agilent) at a flow rate of 0.6 mL/min. The HPLC analysis was performed using a gradient elution method. The mobile phase was composed of a 2 mmol/L ammonium acetate solution (A) and methanol (B). The sample injection volume was 10 μ L. Initially, the mobile phase consisted of 90% eluent A and 10% eluent B. Over the course of 8 minutes, the proportion of eluent A progressively decreased from 90% to 1%, while the proportion of eluent B increased correspondingly. Subsequently, the elution conditions were kept at 1% eluent A and 99% eluent B for 12 minutes. At 12.5 minutes, the gradient was reversed, and the mobile phase composition was gradually adjusted back to the initial conditions (90% eluent A and 10% eluent B) over a specific period.

2. Supplementary Tables

Table S1. Analytical parameter of solid-state ^{13}C NMR spectrum of Py-Azo-COF.

Chemical shift (ppm)	Carbon number	Chemical shift (ppm)	Carbon number
158.93	5	136.10	6.9
151.61	1, 4	128.07	13, 14
143.74	10	112-131	2, 3, 7, 8, ,11, 12

Table S2. Parameters of toxic chemicals.

Toxic chemicals	Molecular Formula	Molecular Mass	Molecular Structure	Abbreviation
Heneicosafluoroundecanoic Acid	$C_{11}HF_{21}O_2$	564.1		PFUNA
Bisphenol A	$C_{15}H_{16}O_2$	228.3		BPA
Tetrabromobisphenol A	$C_{15}H_{12}Br_4O_2$	543.9		TBBPA
Bisphenol S	$C_{12}H_{10}O_4S$	250.3		BPS
Perfluorooctanoic Acid	$C_9HF_{17}O_2$	464.1		PFOA
Myristyltrimethylammonium Bromide	$C_{17}H_{38}BrN$	336.4		TTAB
Nonafluoro-1-butanesulfonic Acid	$CF_3(CF_2)_3SO_3H$	300.1		PFBS

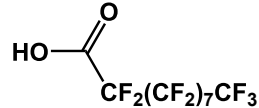
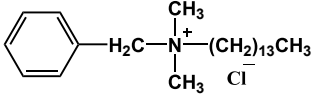
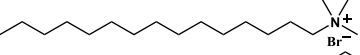
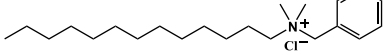
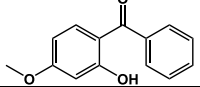
Perfluorocapric Acid	$C_{10}HF_{19}O_2$	514.1		PFDA
Tetradecyldimethylbenzylammonium Chloride	$C_{23}H_{42}ClN \cdot xH_2O$	368.1		TDBAC
Cetyltrimethylammonium Bromide	$C_{19}H_{42}BrN$	364.5		CTAB
Benzalkoniumchloride	$C_{23}H_{42}ClN$	368.0		BAC
2-Hydroxy-4-methoxybenzophenone	$C_{14}H_{12}O_3$	228.0		BP-3

Table S3. RSD values of toxic chemicals by dual-ion-mode SALDI-TOF-MS.

Toxic chemicals	Ion mode	0.1 µg/mL		0.02 µg/mL	
		Shot-to-shot RSD (<i>n</i> = 20) ^a	Sample-to-sample RSD (<i>n</i> = 15) ^b	Shot-to-shot RSD (<i>n</i> = 20) ^a	Sample-to-sample RSD (<i>n</i> = 15) ^b
PFUNA	Negative	26.5%	25.7%	45.3%	47.0%
BPA	Negative	28.5%	29.3%	43.3%	56.2%
TBBPA	Negative	26.3%	29.8%	33.5%	46.6%
BPS	Negative	20.9%	21.9%	49.6%	46.2%
PFOA	Negative	28.7%	28.0%	45.5%	62.2%
TTAB	Positive	12.4%	15.1%	38.5%	37.4%
PFBS	Negative	8.7%	15.5%	19.2%	20.3%
PFDA	Positive	22.8%	28.5%	55.4%	59.6%
TDBAC	Positive	14.2%	15.0%	25.4%	27.3%
CTAB	Positive	5.2%	19.4%	25.5%	36.8%
BAC	Positive	26.2%	29.8%	48.6%	53.4%
BP-3	Positive	24.9%	27.5%	28.1%	30.5%

^a The shot-to-shot RSDs were measured based on 20 shots at different locations on the MALDI target (*n* = 20).

^b The sample-to-sample RSDs were measured based on 15 samples in different batches (*n* = 15).

Table S4. Analytical parameter of trace toxic chemicals by dual-ion-mode SALDI-TOF-MS.

Toxic chemicals	Ion mode	m/z^a	LOD (pg/mL) ^b	Linear range (µg/mL)	Calibration equation	R^2
PFUNA	Negative	562.4	0.02	0.02-0.2	$y = 5.4 \times 10^4 x + 5.4 \times 10^3$	0.940
BPA	Negative	226.7	0.01	0.002-0.2	$y = 1.5 \times 10^6 x + 5.1 \times 10^3$	0.992
TBBPA	Negative	542.4	0.2	0.002-2	$y = 1.2 \times 10^3 x + 1.7 \times 10^3$	0.956
BPS	Negative	248.7	0.01	0.002-0.2	$y = 1.1 \times 10^6 x + 4.4 \times 10^2$	0.967
PFOA	Negative	462.4	0.2	0.002-2	$y = 1.4 \times 10^3 x + 5.7 \times 10^3$	0.962
TTAB	Positive	256.1	0.005	0.002-0.1	$y = 2.0 \times 10^7 x - 8.8 \times 10^4$	0.938
PFBS	Negative	298.6	0.002	0.002-0.2	$y = 9.2 \times 10^6 x + 8.4 \times 10^5$	0.923
PFDA	Positive	513.9	0.2	0.002-0.2	$y = 3.8 \times 10^5 x + 5.0 \times 10^4$	0.944
TDBAC	Positive	332.2	0.002	0.002-0.2	$y = 4.0 \times 10^6 x + 3.0 \times 10^5$	0.915
CTAB	Positive	284.9	0.002	0.0002-0.02	$y = 4.1 \times 10^7 x + 1.0 \times 10^6$	0.916
BAC	Positive	332.2	0.01	0.002-0.2	$y = 2.4 \times 10^6 x - 2.5 \times 10^4$	0.946
BP-3	Positive	228.9	0.01	0.002-0.1	$y = 4.5 \times 10^4 x + 1.7 \times 10^3$	0.927

Note. Standard curve was utilized to quantify the target toxic chemical. Standard solutions with concentrations ranging from 0.2 ng/mL to 200 µg/mL of trace-level toxic chemicals were prepared to establish the curve. The curve was established by measuring the peak intensity of a standard sample using Py-Azo-COF as a SALDI probe.

^a The m/z values of the MS peaks used in quantitative analysis.

^b The LOD was determined by gradually diluting the standard sample and assessing the S/N ratio. The LOD was defined as the minimum concentration value from three parallel samples that could generate a reliable measurement signal ($S/N > 3$).

Table S5. Comparison of analytical performance of different materials as SALDI probes.

Nanomaterial	Sample	Analyte	LOD	RSD	Reference
Graphene oxide nanoribbons	Wastewater	BDE-47 and TBBPA	3.3-4.4 ng/mL	1.7%-22.3%	1
Fluorographene	Paper products; canned food and sewage sludge	Emerging chemical contaminants (such as TDBAC, TBBPA and E2)	6.0×10^{-6} -0.50 ng/mL	11.1%-32.3%	2
Aminated graphene	Ultrapure water	Typical chemical contaminants (such as BPS, BDE-47 and PCP)	$0.1-5.0 \times 10^3$ ng/mL	7.2%-52.7%	3
Carboxylated graphene	Ultrapure water	Typical chemical contaminants (such as E2, TBBPA and TDBAC)	$0.1-5.0 \times 10^3$ ng/mL	5%-38.0%	3
Oxidized graphene	Ultrapure water	Typical chemical contaminants (such as DDBAC, CTAB and TTAB)	$1-5.0 \times 10^4$ ng/mL	33.3%-77%	3
Self-assembly TiO ₂ nanosheets	Pollution water	PFOS	10 ng/mL	7.29%-17.37%	4
Polydopamine nanospheres	PM _{2.5}	PAHs, BPs, BzPs, PFCs and Es	1.0×10^{-7} - 1.0×10^4 ng/mL	—	5
C60-functionalized magnetic silica microsphere	Water and human urine	Peptides and proteins	200 ng/mL	—	6

Fe ₃ O ₄ @BTA-DHBD	Pharmaceuticals and personal care products	Bisphenols	5.0×10 ⁻² -4.0×10 ³ ng/mL	5%-12%	7
CeO ₂ -CB	Mineral water and soft drink	Pharmaceutical drugs	1.0×10 ² ng/mL	1.8%	8
Py-Azo-COF	Wastewater and sewage sludge	Trace toxic chemicals	2.0×10 ⁻³ -0.20 ng/mL	5.2%-29.8%	This work

Abbreviations: BTA: benzene-1,3,5-tricarbaldehyde; DHBD: 3,3'-dihydroxybenzidine; CB: carbon black; BDE-47: 2,2',4,4'-Tetrabromodiphenyl ether; TBBPA: tetrabromobisphenol A; PCP: organochlorine pesticide; E2: estradiol; DDBAC: dodecyldimethylbenzylammonium chloride; PFOS: perfluorooctanesulfonic acid; PAHs: polycyclic aromatic hydrocarbons; BPs: bisphenols; BzPs: benzodiazepine; PFCs: perfluorobutyric acid; Es: estrogens; LOD: limit of detection.

Table S6. Comparison of analytical performance of different techniques for the analysis of toxic chemicals.

Method	Sample	Pretreatment	Analyte	LOD	Reference
GC-TOF-MS	Wastewater	SPE (Strata X)	UV-filters	1.0-5.0 ng/L	9
GC-HRMS	Wastewater	LLE; SPE (Florisil column)	EOCs	3.2-44 ng/L	10
UPLC-ESI-MS	Surface waters	SPE (MWCNTs)	PFOA and PFOS	10-15 ng/L	11
LC-MS	Seawater and river water	SPE (HR-X)	Pharmaceuticals	1.0-50 ng/L	12
LC-UV	Seawater, river water and swimming pool water	DLLME	UV-filters	1.9-6.4 ng/L	13
UFLC-FLD	Seawater	SPE (C18)	BPA, 4NNP, 4NOP, 4TOP, E3, E1, E2 and EE2	0.40-5.6×10 ³ ng/L	14
HPLC-HRMS	Freshwater invertebrates	SPE (C18)	PPCPs	0.04-2.38 ng/g	15
SALDI-TOF MS	Wastewater and sewage sludge	Py-Azo-COF	Trace toxic chemicals	2.0×10 ⁻³ -0.20 ng/L	This work

Abbreviations: GC: gas chromatography; TOF: Time-of-flight; MS: mass spectrometry; HRMS: high-resolution mass spectrometry; UPLC: ultra-performance liquid chromatography; ESI: electrospray ionization; UFLC: ultra-fast liquid chromatography; FLD: fluorescence detector; SPE: solid-phase extraction; MWCNTs: multiwalled carbon nanotubes; DLLME: dispersive liquid-liquid microextraction; EOCs: estrogenic organic contaminants; PFOS: perfluorooctane

sulfonate; PFOA: perfluorooctanoic acid; BPA: bisphenol A; 4NNP: 4-n-nonylphenol; 4NOP: 4-n-octylphenol; 4TOP: 4-t-octylphenol; E3: estriol; E1: estrone; E2: 17 β -estradiol; EE2: 17 α -ethynylestradiol; PPCPs: pharmaceutical and personal care products.

Table S7. Molecular docking of Py-Azo-COF with different trace toxic chemicals.

Trace toxic chemicals	Binding energy score (kcal·mol⁻¹)	Binding sites with hydrogen-bond	Binding sites with hydrophobic interaction	Binding sites with electrostatic interaction	Binding sites with π-π interaction	Binding sites with π-sulfur bond
BPA	-37.83	-OH	/	/	Benzene ring	/
CTAB	-288.20	/	Alkyl group	Ammonium group	/	/
TDBAC	-242.71	/	Alkyl group	Ammonium group	/	/
PFBS	-79.41	/	/	Sulfonic acid	/	Sulfonic acid

Table S8. Recovery of toxic chemicals in wastewater and sewage sludge by dual-ion-mode SALDI-TOF-MS.

Toxic chemicals	Ion mode	Recovery (Wastewater)	Recovery (Sewage sludge)
PFUNA	Negative	139.4%	27.3%
BPA	Negative	45.5%	83.5%
TBBPA	Negative	88.7%	102.8%
BPS	Negative	72.5%	59.8%
PFOA	Negative	26.3%	77.9%
TTAB	Positive	99.7%	98.0%
PFBS	Negative	123.1%	118.9%
PFDA	Positive	58.7%	60.0%
TDBAC	Positive	52.2%	75.8%
CTAB	Positive	99.9%	96.7%
BAC	Positive	127.6%	169.7%
BP-3	Positive	122.7%	83.4%

Table S9. RSD values of toxic chemicals in the real samples by dual-ion-mode SALDI-TOF-MS.

Toxic chemicals	Ion mode	RSD (Wastewater)		RSD (Sewage sludge)	
		Shot-to-shot RSD ($n = 20$) ^a	Sample-to-sample RSD ($n = 15$) ^b	Shot-to-shot RSD ($n = 20$) ^a	Sample-to-sample RSD ($n = 15$) ^b
PFUNA	Negative	29.4%	28.1%	34.5%	30.1%
BPA	Negative	25.1%	24.2%	31.2%	32.9%
TBBPA	Negative	35.2%	38.1%	38.5%	39.1%
BPS	Negative	29.8%	26.7%	24.5%	31.2%
PFOA	Negative	24.2%	30.1%	30.1%	35.1%
TTAB	Positive	19.4%	20.3%	14.2%	17.9%
PFBS	Negative	11.3%	14.1%	19.5%	20.3%
PFDA	Positive	36.7%	33.2%	38.9%	36.9%
TDBAC	Positive	16.9%	17.9%	24.1%	29.4%
CTAB	Positive	19.4%	20.5%	14.5%	19.8%
BAC	Positive	29.4%	26.9%	30.4%	29.1%
BP-3	Positive	33.4%	31.1%	35.2%	33.7%

Note: The RSD value of the Py-Azo-COF probe was usually higher in the real sample (wastewater and sewage sludge) than in the ultrapure water sample, which indicated that the substrate in the real sample will interfere with the detection ability of the Py-Azo-COF probe. Therefore, in order to improve the performance of the Py-Azo-COF probe in the real sample, it can be considered to concentrate or pretreat the real sample to remove the possible substrate. Analyte concentration: 0.1 µg/mL.

^a The shot-to-shot RSDs were measured based on 20 shots at different locations on the MALDI target ($n = 20$).

^b The sample-to-sample RSDs were measured based on 15 samples in different batches ($n = 15$).

Table S10. Concentration of perfluorinated compounds in wastewater and sewage sludge samples detected by HPLC-ESI MS.

Toxic chemicals	Molecular Mass	Wastewater (ng/L)	Sewage sludge (ng/L)
PFUNA	564.1	0.0070-0.44	0.0029-0.0059
PFDA	514.1	0.05-4.1	0.0080-0.026
PFBS	300.1	0-2.85	0-0.79
PFOA	464.1	0.0011-0.0088	0.0080-0.026
PFBA	214.0	0.015-0.14	0.091-0.40
PFPeA	264.0	5.90-45.19	0-12.15
PFHpA	364.1	1.27-14.87	0.27-0.68
PFHxA	314.1	0-0.013	0-0.027
PFTTrDA	664.1	0.35-0.47	0.37-0.70
FOSA	499.1	0.077-0.12	0.074-0.094
PFHxS	400.1	0.0070-0.0072	0.0070-0.0071
PFOS	500.1	0-11.69	0-8.15
PFTeDA	714.1	ND	0-0.54

Note. ND: Below the detection limit.

Abbreviations: PFBA: heptafluorobutyric acid; PFPeA: perfluorovaleric acid; PFHpA: perfluoroheptanoic acid; PFHxA: perfluorohexanoic acid; PFTTrDA: perfluorotetradecanoic acid; FOSA: perfluorooctanesulfonamide; PFHxS: perfluorohexanesulfonic acid; PFOS: heptadecafluorooctanesulfonic acid.

3. Supplementary Figures

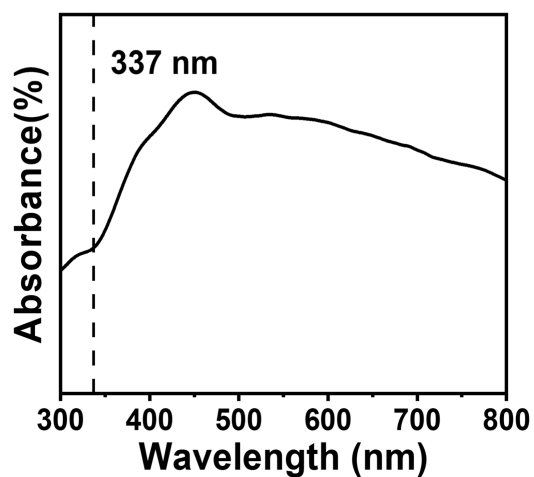


Fig. S1. UV-visible absorption spectra of Py-Azo-COF.

Note: The absorption of Py-Azo-COF at the MALDI laser wavelength (337 nm) suggests its potential as a MALDI matrix. This characteristic enables it to effectively absorb laser energy, facilitating the ionization and desorption of the target analytes in MALDI detection.

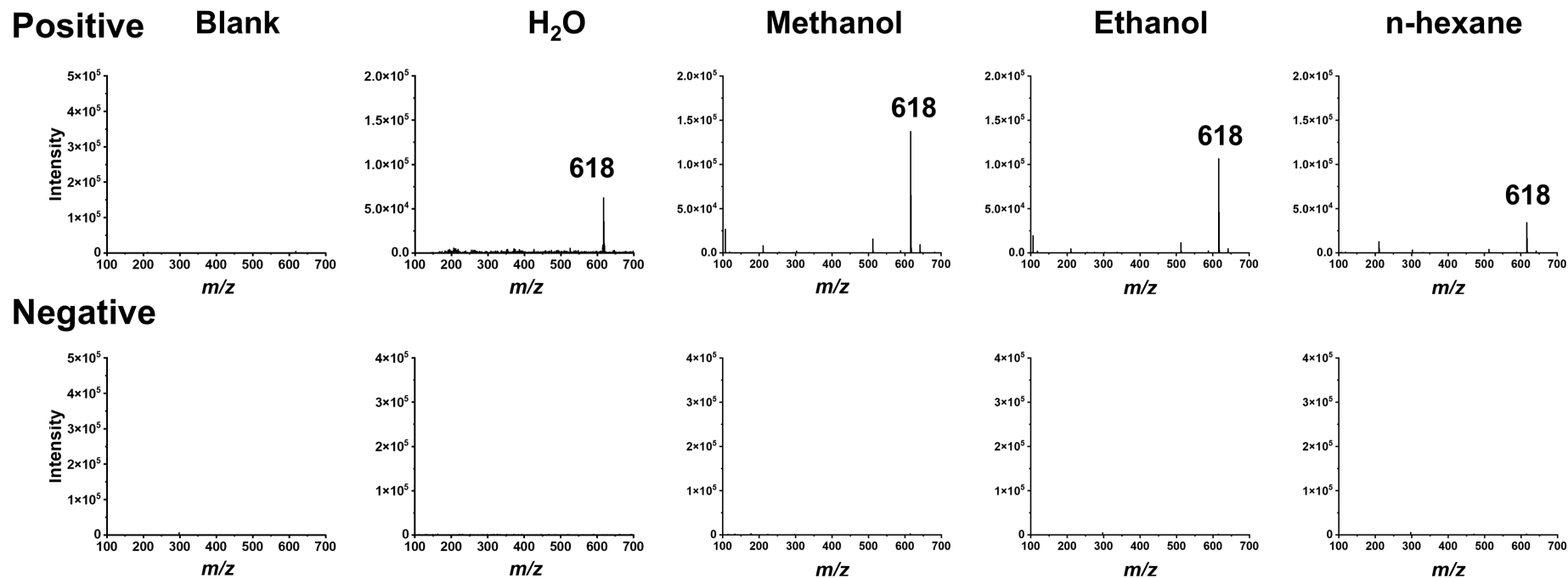


Fig. S2. MALDI-TOF MS of blank sample and Py-Azo-COF under different dispersants (*i.e.*, methanol, n-hexane, ethanol, and H₂O) in dual-ion-mode.



Methanol

n-hexane

Ethanol

H₂O

Fig. S3. The Py-Azo-COF dispersion in various dispersants (methanol, n-hexane, ethanol, and H₂O). The dispersion of Py-Azo-COF varies depending on the dispersant used. Methanol and H₂O were the most effective solvents, leading to a uniformly dispersed suspension of Py-Azo-COF in a short period. Ethanol showed poor dispersion, with some precipitation still visible after 30 minutes of ultrasonic treatment. N-hexane, on the other hand, had the least effective dispersion, making it difficult for Py-Azo-COF to form a suspension. Concentration: 1 mg/mL.

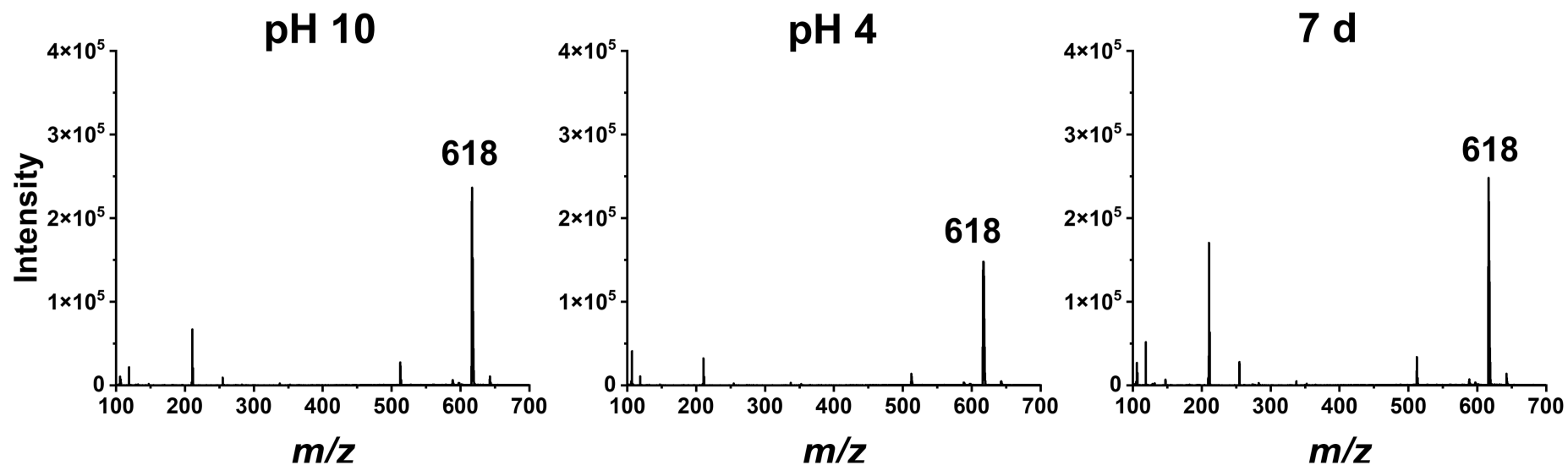


Fig. S4. Mass spectra of Py-Azo-COF were obtained under different conditions (acidic and alkaline solutions) at ambient temperature for 7 days using positive ion mode LDI-TOF MS. Py-Azo-COF ($m/z = 618$) showed excellent stability, as confirmed by its detectability using MALDI-TOF MS under different conditions.

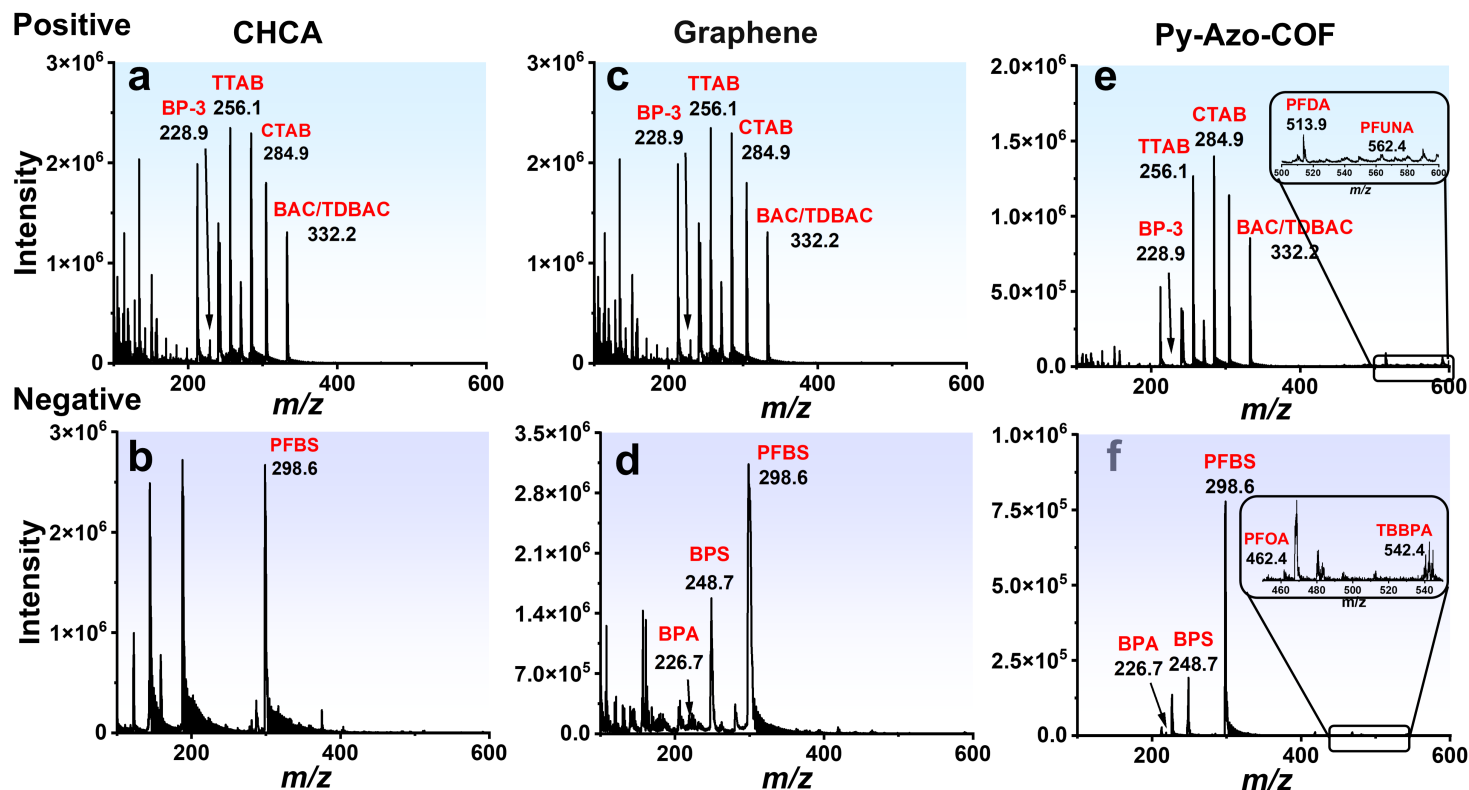


Fig. S5. Comparison of MS performance of different materials as MALDI matrices in dual-ion-mode MALDI-TOF MS for detecting typical toxic chemicals (PFOA, PFBS, PFUNA, PFDA, BPA, BPS, TTBPA, BAC, CTAB, TTAB, TDBAC, and BP-3). The top (a, c, e) and bottom (b, d, f) represent the spectra obtained in positive and negative ion mode, respectively. The matrices include (a-b) CHCA, (c-d) graphene, and (e, f) Py-Azo-COF. Analyte concentration: 42 $\mu\text{g/mL}$. Using Py-Azo-COF as a MALDI matrix allowed the detection of all selected toxic chemicals with extremely low background interference in the low-mass regions. When using CHCA as a MALDI matrix, only six target analytes were detected. In particular, in the negative ion mode, only the $[\text{M} - \text{H}]^-$ peak of PFBS was detected. Furthermore, strong background interference was observed in the low molecular mass range. In the case of graphene as a MALDI matrix, eight target analytes could be detected by MALDI-TOF MS. For example, the peaks of $[\text{M} - \text{Br}]^+$ of CTAB and TTAB in the positive ion mode and $[\text{M} - \text{H}]^-$ of PFBS in the negative ion mode exhibited strong intensity. There was background interference in the low-mass region.

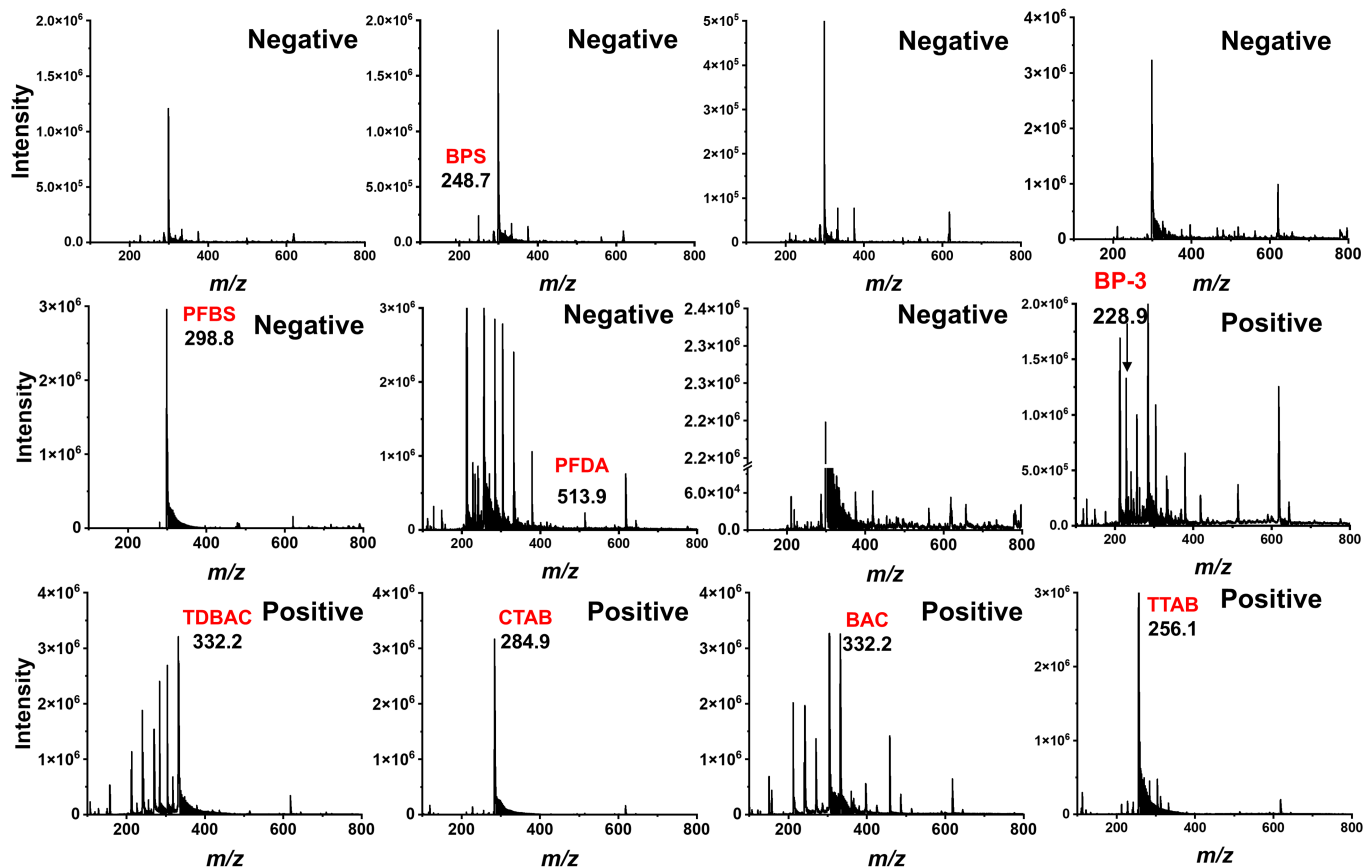


Fig. S6. Mass spectra of toxic chemicals using CHCA as a SALDI probe by dual-ion mode LDI-TOF MS. The figure represents the spectra obtained in negative and positive ion mode, respectively. Analyte concentration: 200 $\mu\text{g/mL}$. The mass spectra verified that the chemical structure of trace toxic chemicals affected the MS fingerprints. By utilizing CHCA as a SALDI probe, only eight trace toxic compounds were detectable in the presence of the toxic compound standards alone. When dealing with mixed standards, the detection capacity may be further reduced, suggesting that CHCA might be not suitable as a matrix for detecting small molecular toxic compounds.

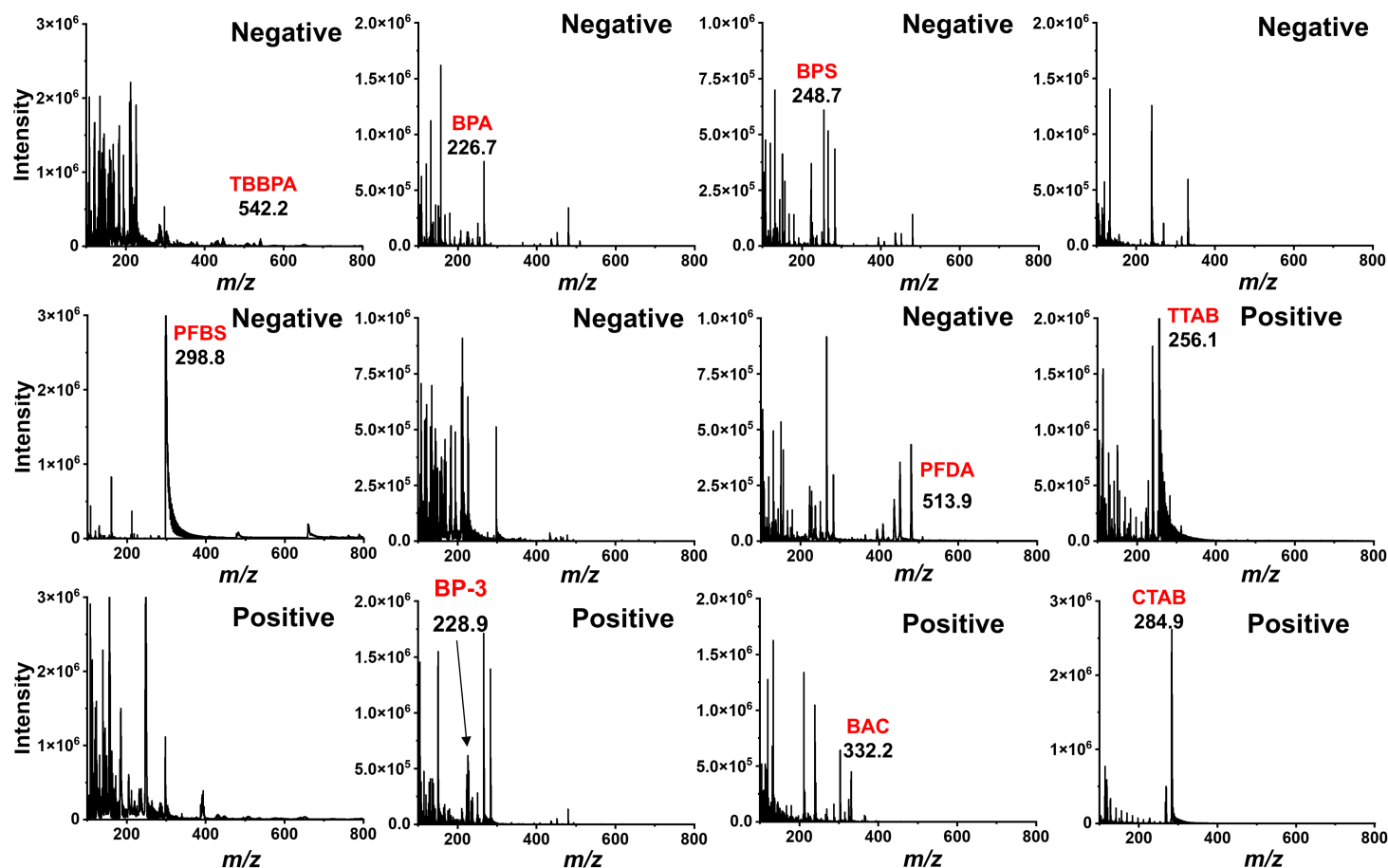


Fig. S7. Mass spectra of toxic chemicals using graphene as a SALDI probe by dual-ion mode LDI-TOF MS. The figure represents the spectra obtained in negative and positive ion mode, respectively. Analyte concentration: 200 $\mu\text{g/mL}$. The use of graphene as a SALDI probe allowed for the detection of nine toxic compounds individually. However, significant background interference was observed, potentially attributed to carbon cluster peaks generated by graphene in the low molecular mass region. This result highlights the challenges associated with achieving effective enrichment and screening of low molecular mass target compounds using graphene.

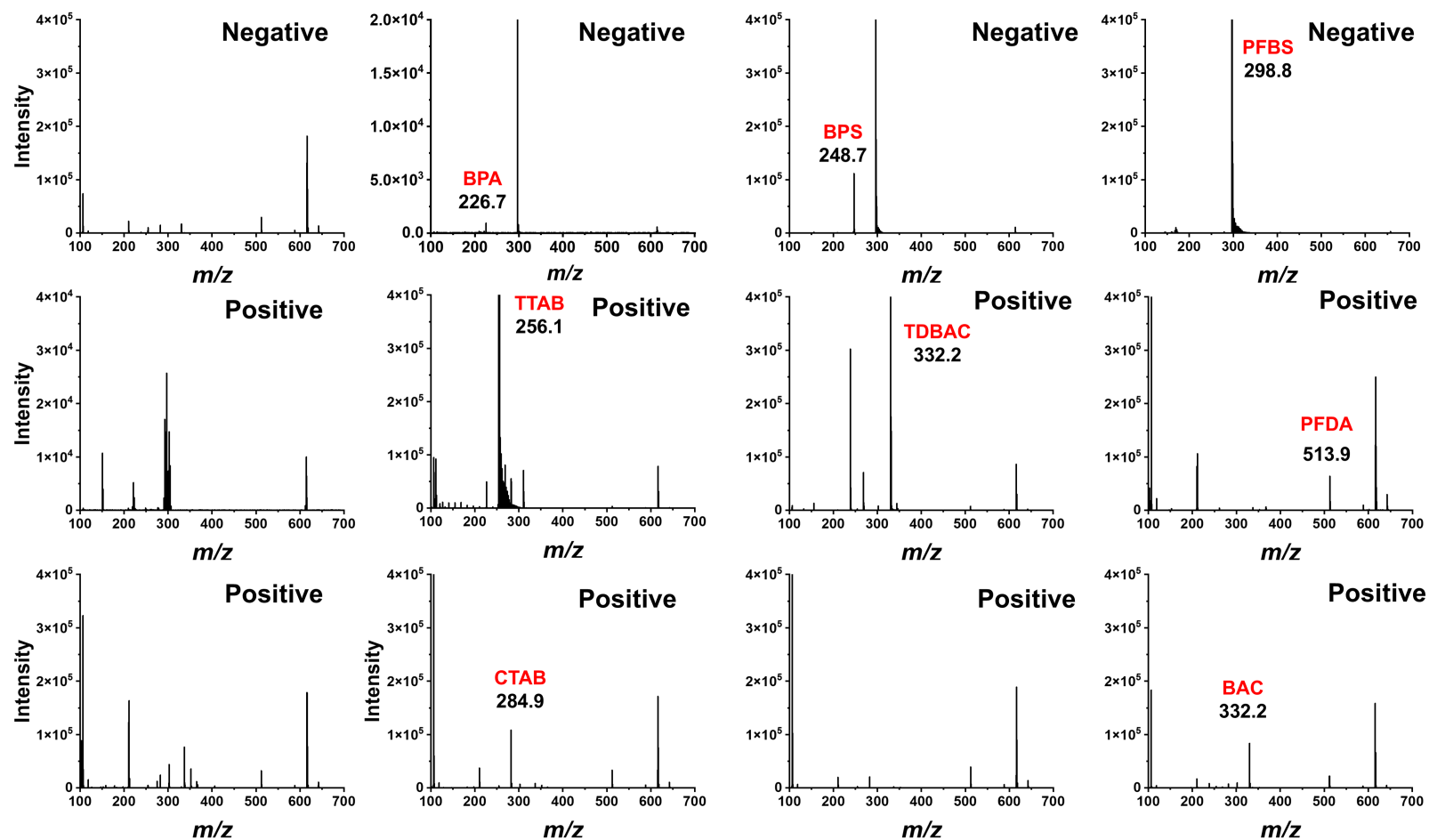


Fig. S8. Mass spectra of toxic chemicals using Py-Azo-COF as a SALDI probe within 0 hour using dual-ion mode LDI-TOF MS. The figure represents the spectra obtained in negative and positive ion mode, respectively. The concentration of the analyte was 200 $\mu\text{g/mL}$. The mass spectra verified that the chemical structure of toxic chemicals affected the MS fingerprints. By utilizing Py-Azo-COF as a SALDI probe in 0 hour, only eight trace toxic chemicals were detectable in the presence of the toxic compound standard alone. The peak intensity of the target trace toxic compounds is low.

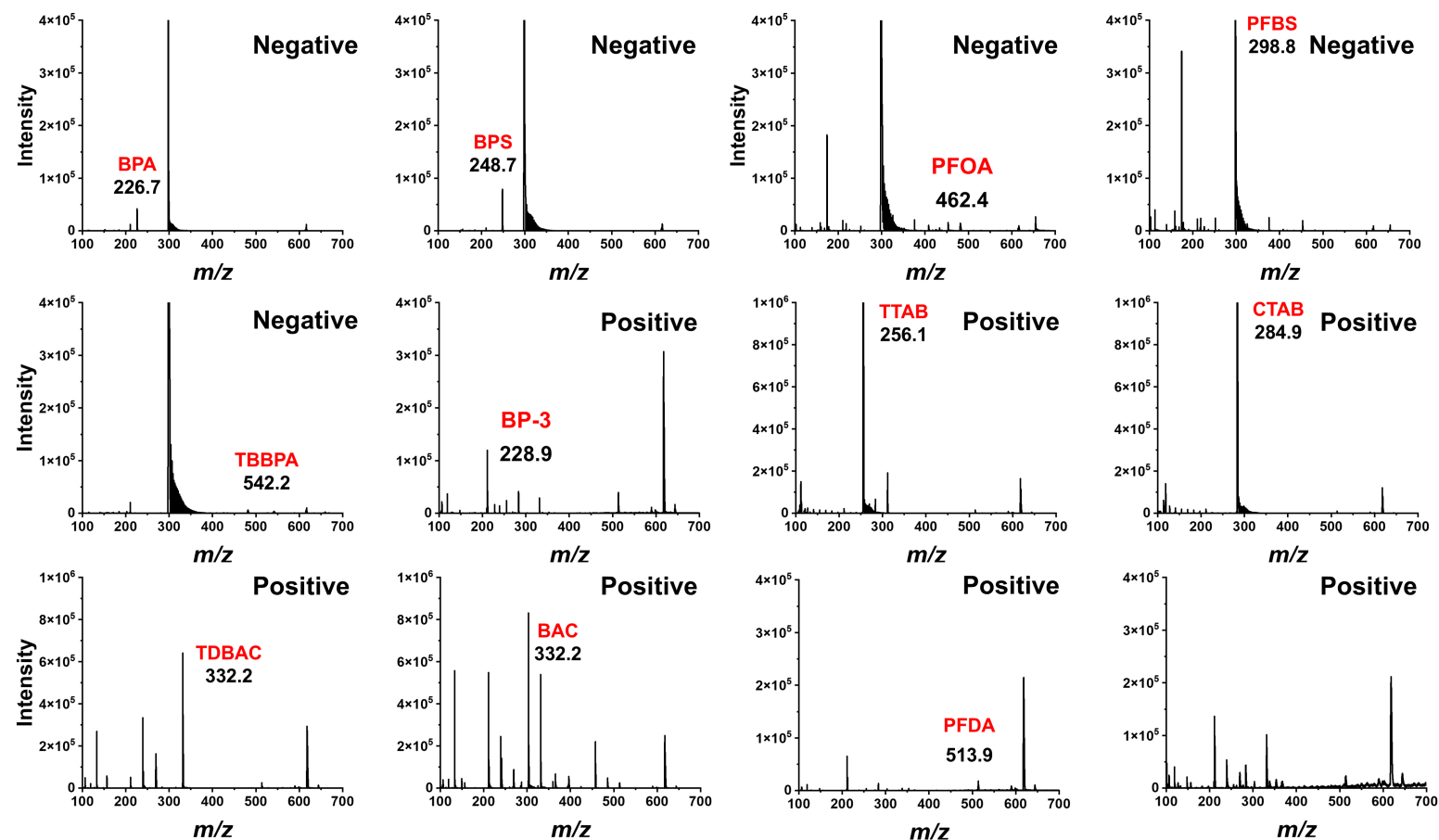


Fig. S9. Mass spectra of toxic chemicals using Py-Azo-COF as a SALDI probe within 4 hours using dual-ion mode LDI-TOF MS. The figure represents the spectra obtained in negative and positive ion mode, respectively. Analyte concentration: 200 $\mu\text{g/mL}$. The mass spectra confirmed that the chemical structure of trace toxic chemicals influenced the MS fingerprints. By utilizing Py-Azo-COF as a SALDI probe for 4 hours, only nine trace toxic chemicals were detectable in the presence of the toxic compound standards alone. The peak intensity of the toxic compounds in the target is higher than that of the 0-hour incubation result. However, the 4-hour incubation period does not meet the detection requirements.

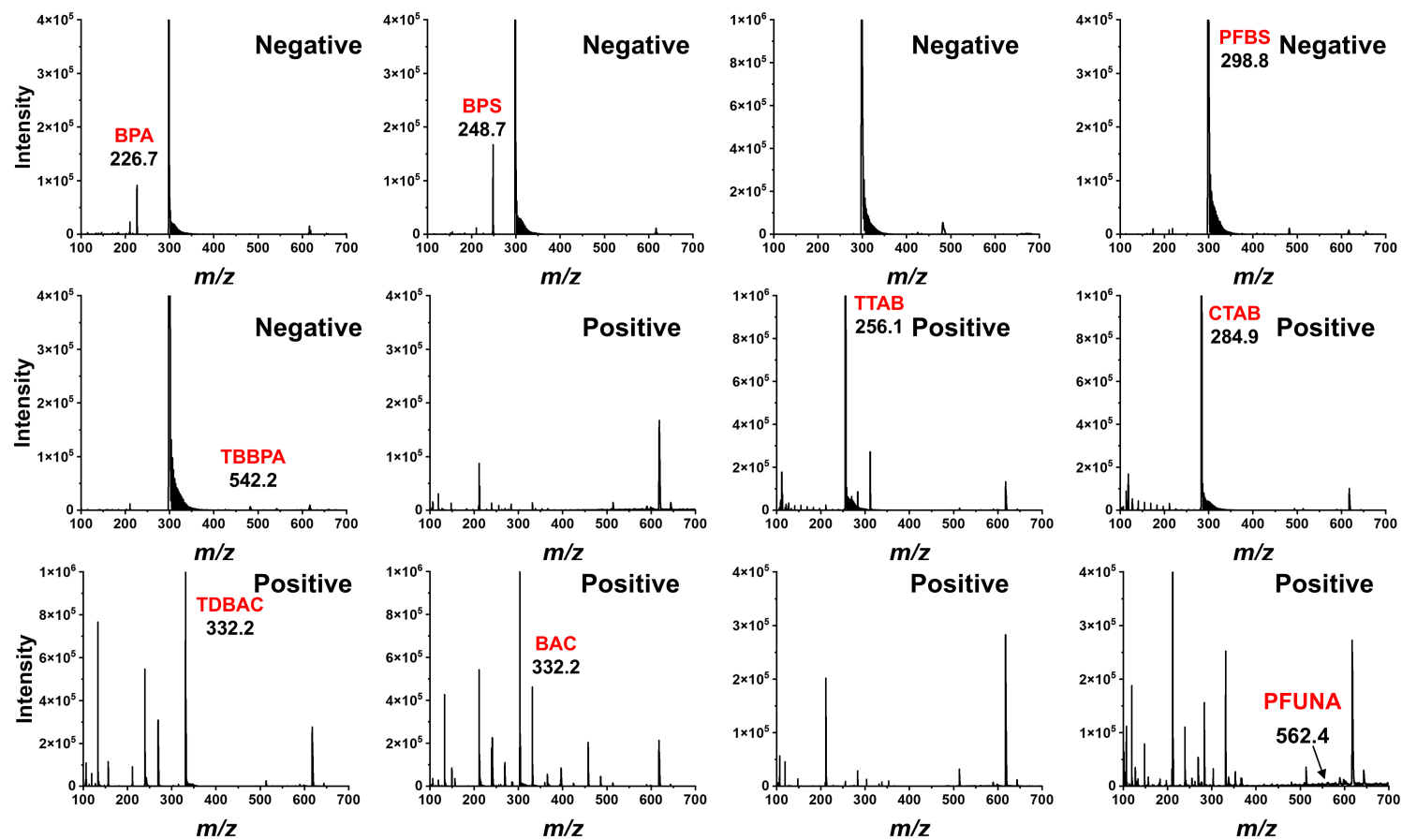


Fig. S10. Mass spectra of toxic chemicals using Py-Azo-COF as a SALDI probe in 12 hours by dual-ion mode LDI-TOF MS. The figure represents the spectra obtained in negative and positive ion mode, respectively. Analyte concentration: 200 $\mu\text{g/mL}$. The mass spectra verified that the chemical structure of trace toxic chemicals affected the MS fingerprints. By using Py-Azo-COF as a SALDI probe for 12 hours, eleven trace toxic chemicals were detectable in the presence of the toxic compound standards alone. The peak intensity of the toxic compounds is higher than the result of 4-hour incubation. But BP-3 was not detected after 12 hours, suggesting that Py-Azo-COF needed more time to enrich BP-3. Consequently, we extended the incubation period to 24 hours.

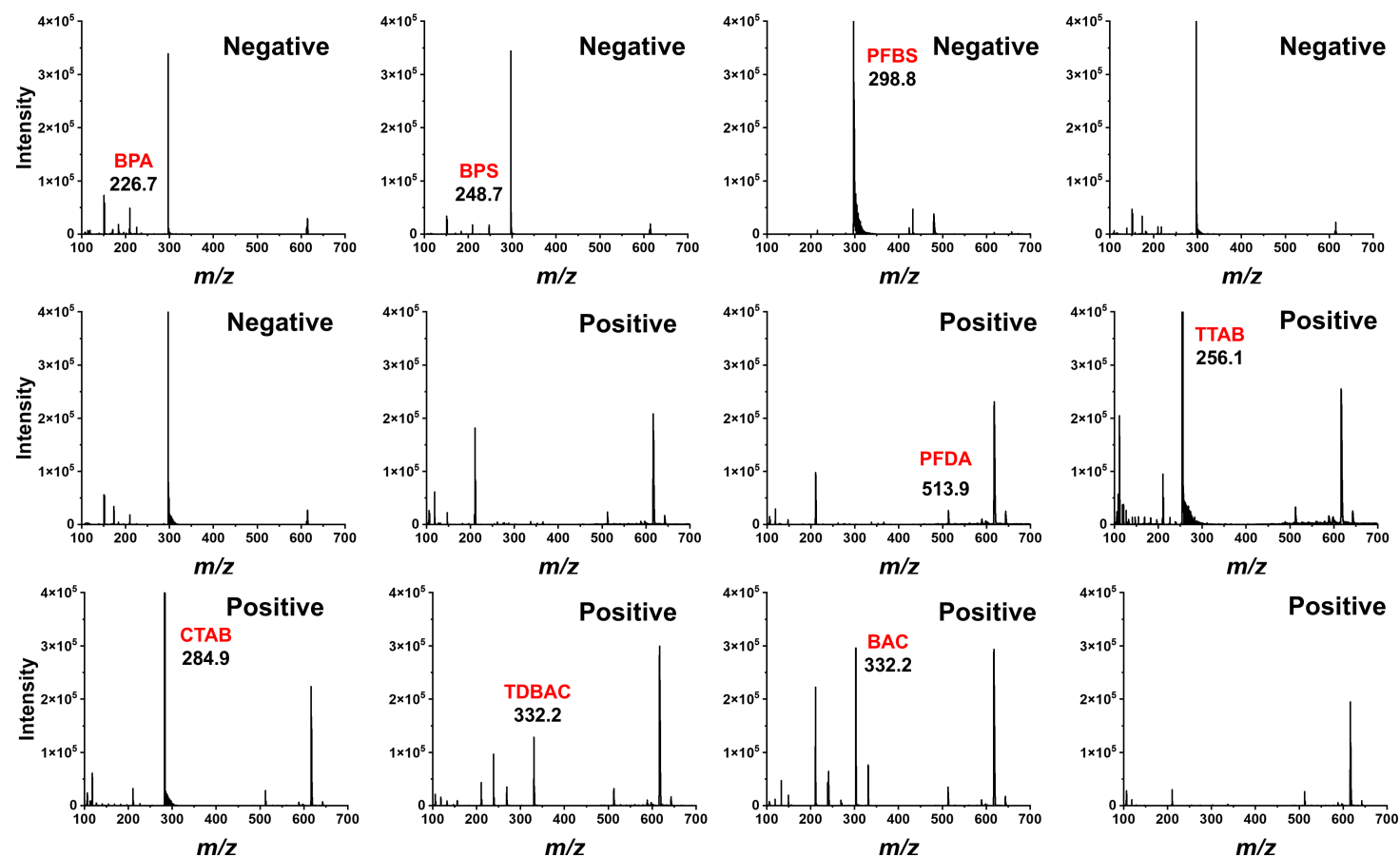


Fig. S11. Mass spectra of toxic chemicals using Py-Azo-COF as a SALDI probe in methanol by dual-ion mode LDI-TOF MS. The figure represents the spectra obtained in negative and positive ion mode, respectively. Analyte concentration: 200 $\mu\text{g/mL}$. The mass spectra verified that the chemical structure of trace toxic chemicals affected the MS fingerprints. Py-Azo-COF was dispersed in methanol and used as the SALDI probe for MS analysis. While the dispersion of Py-Azo-COF in methanol was better, only eight toxic chemicals were detected under the same experimental conditions, showing lower peak intensities compared to when H_2O was used as the dispersant.

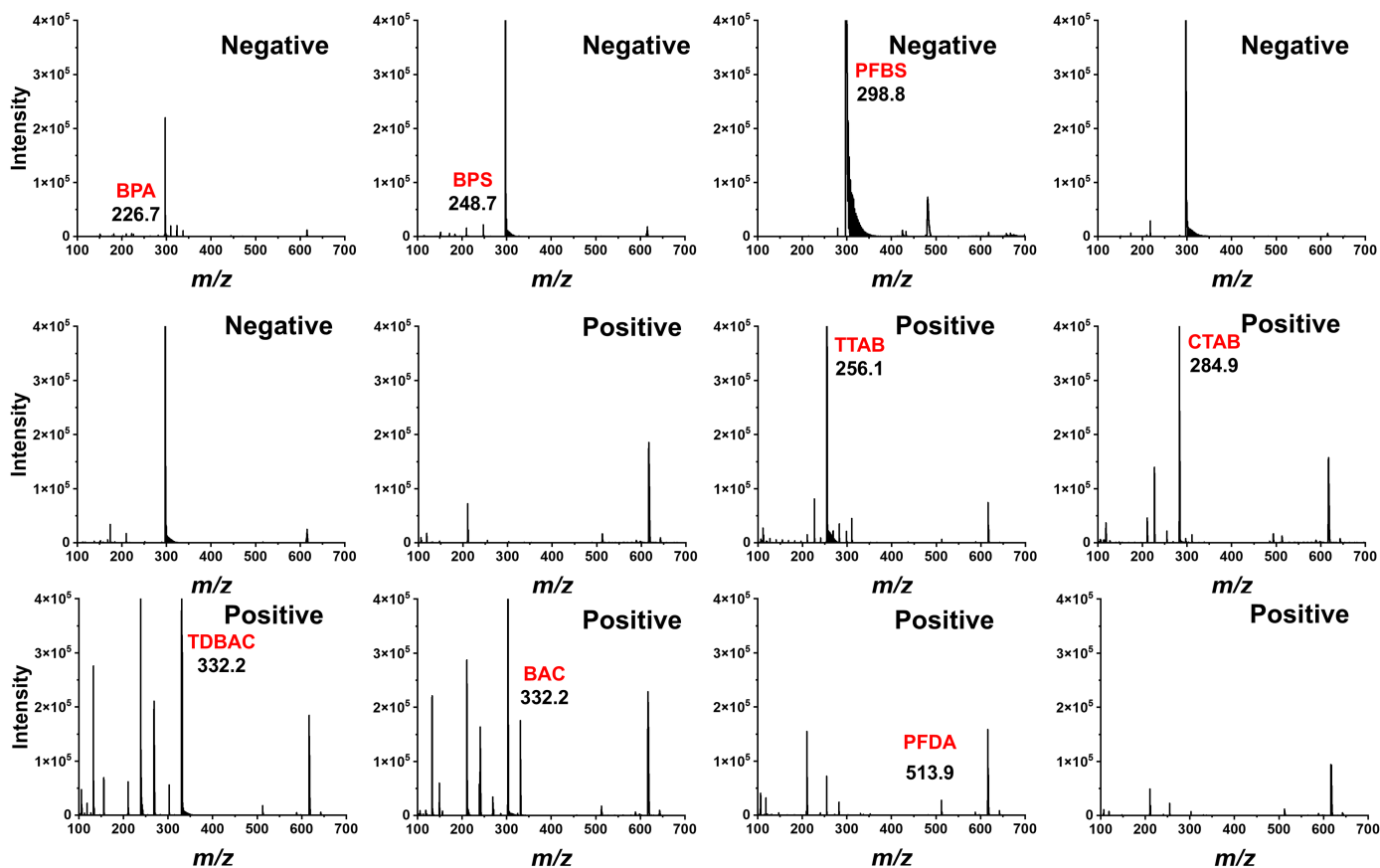


Fig. S12. Mass spectra of toxic chemicals using Py-Azo-COF as a SALDI probe in n-hexane by dual-ion mode LDI-TOF MS. The figure represents the spectra obtained in negative and positive ion mode, respectively. Analyte concentration: 200 $\mu\text{g/mL}$. Py-Azo-COF was dispersed in n-hexane and used as the SALDI probe for MS analysis. Py-Azo-COF showed poor dispersion in n-hexane, making it unsuitable as a dispersant. However, we still used it for MS analysis as a SALDI probe in n-hexane. Nine target toxic compounds were detected, but the peak intensity was lower compared to when H_2O was used as the dispersant.

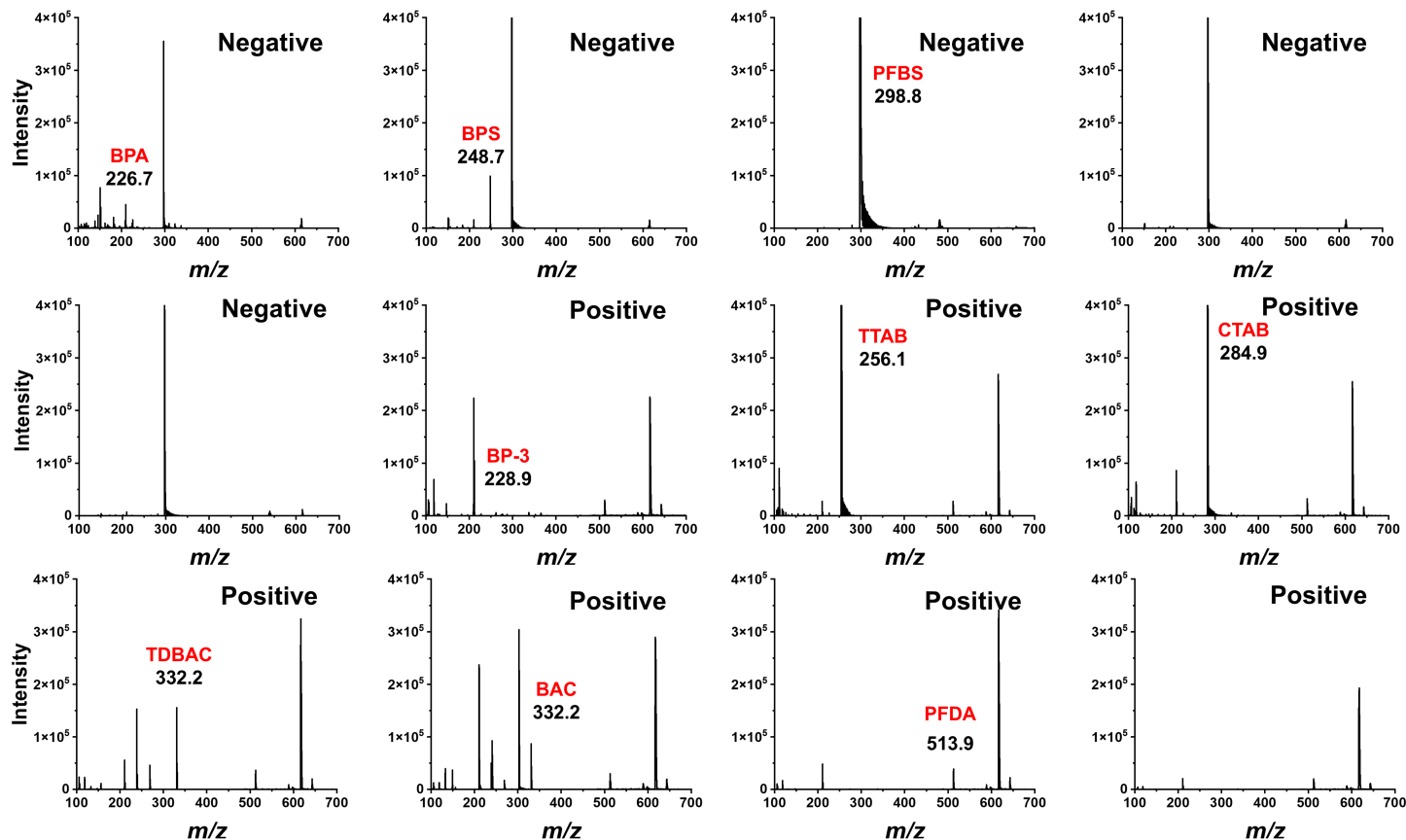


Fig. S13. Mass spectra of toxic chemicals using Py-Azo-COF as a SALDI probe in ethanol by dual-ion mode LDI-TOF MS. The figure represents the spectra obtained in negative and positive ion mode, respectively. Analyte concentration: 200 $\mu\text{g/mL}$. The mass spectra verified that the chemical structure of trace toxic chemicals affected the MS fingerprints. Py-Azo-COF was dispersed in ethanol and used as the SALDI probe for MS analysis. The dispersion of Py-Azo-COF in ethanol is slightly less effective than the dispersion of H_2O . Only eight target toxic compounds were detected under the same experimental conditions, showing significantly lower peak intensities compared to when H_2O was used as the dispersant.

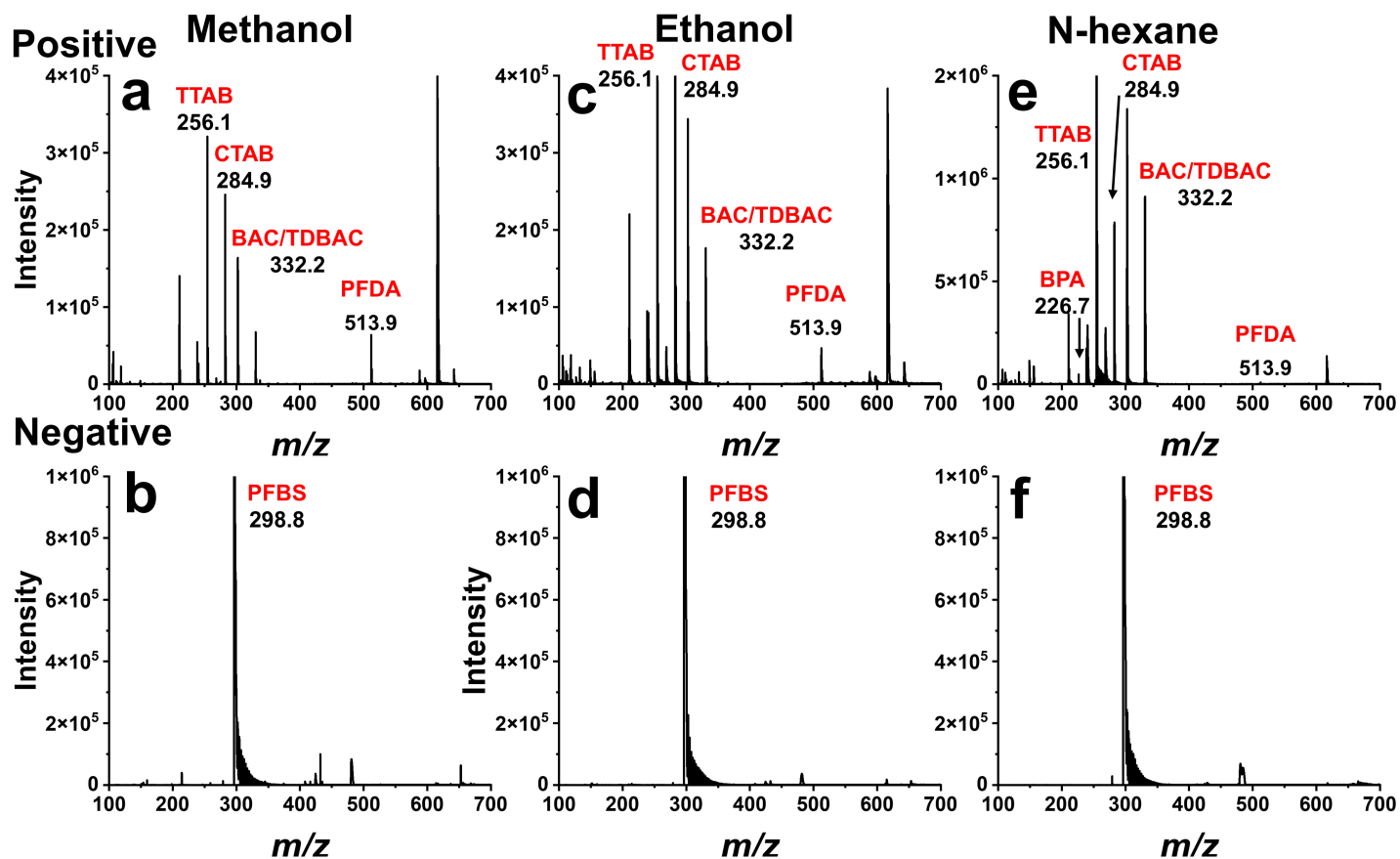


Fig. S14. Mass spectra of twelve toxic chemicals using Py-Azo-COF as a SALDI probe in different solutes (methanol, n-hexane and ethanol) by dual-ion mode LDI-TOF MS. The top (a, c, e) and bottom (b, d, f) represent the spectra obtained in positive and negative ion mode, respectively. Analyte concentration: 33 $\mu\text{g/mL}$. A mixture of twelve toxic compounds was added to different solvents (methanol, n-hexane and ethanol). Six trace toxic chemicals were detected in both methanol and ethanol, while seven toxic chemicals were detected specifically in n-hexane. Different toxic compounds may interact with each other during the Py-Azo-COF enrichment process, leading to a decrease in the detectable compounds when multiple substances are present. It is important to note that the detection efficiency of methanol, ethanol, and n-hexane as dispersants is significantly lower than that of H_2O .

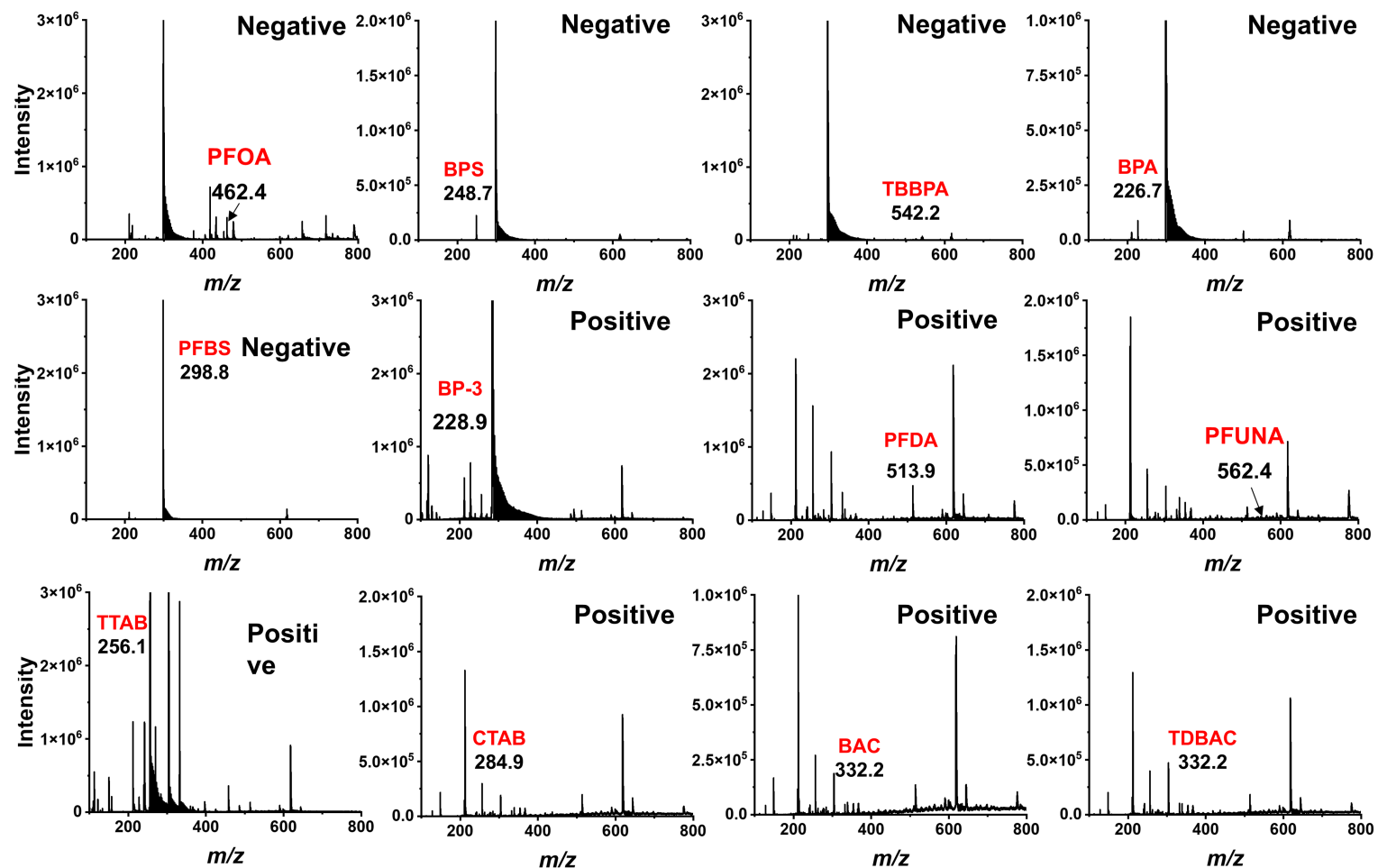


Fig. S15. Mass spectra of toxic chemicals using Py-Azo-COF as a SALDI probe by dual-ion mode LDI-TOF MS. The figure represents the spectra obtained in negative and positive ion mode, respectively. Analyte concentration: 200 $\mu\text{g/mL}$. Using Py-Azo-COF as a SALDI probe, we successfully detected twelve toxic compounds without significant background interference. This observation indicates the excellent performance of Py-Azo-COF as a SALDI probe. However, it was important to note that certain toxic compounds, such as perfluorinated compounds, exhibited low peak intensities. This can be attributed to their intrinsic structural characteristics and the interaction between Py-Azo-COF and perfluorinated compounds.

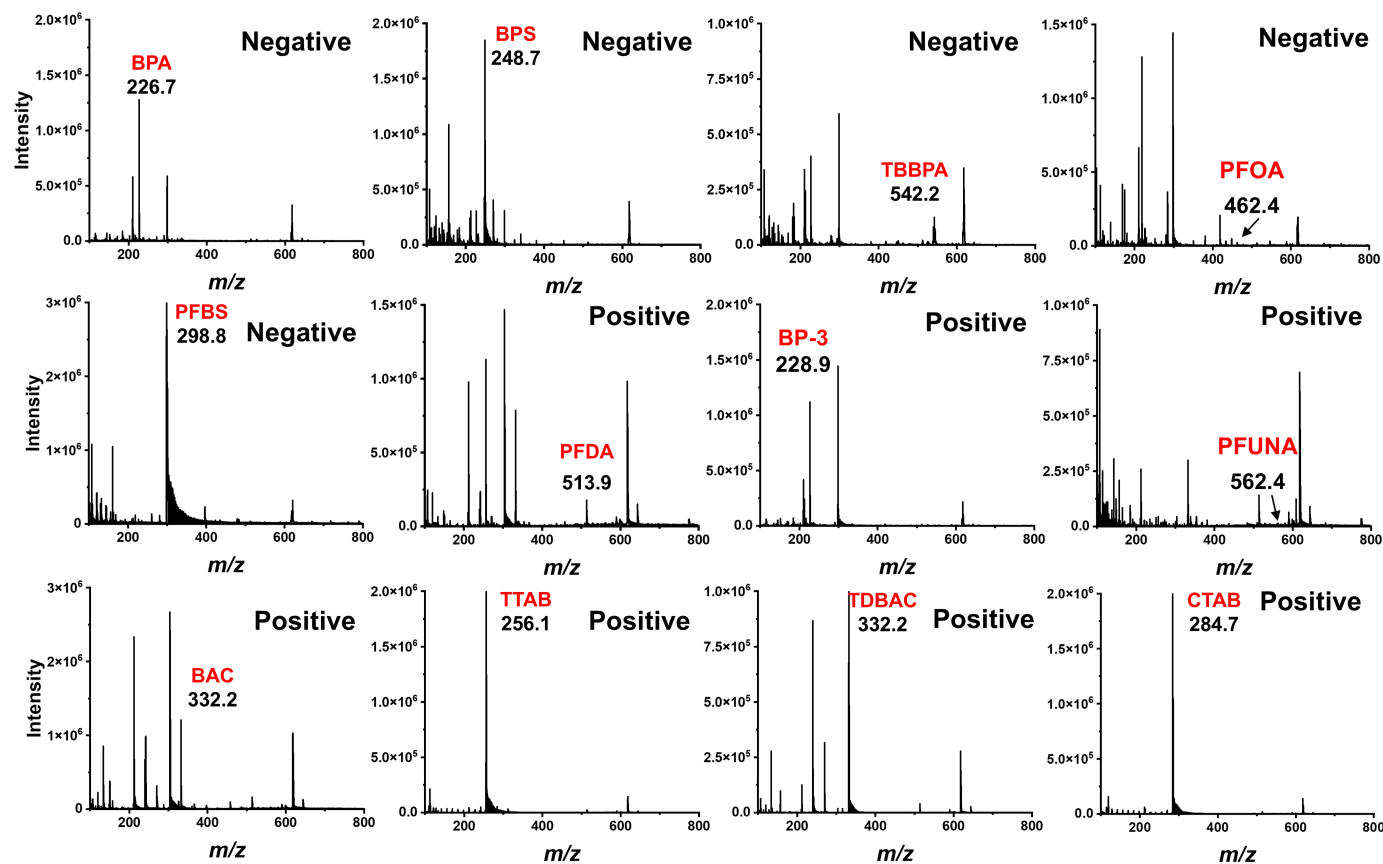


Fig. S16. Effect of environmental factor (*i.e.*, humic acid) on MS performance of Py-Azo-COF as a SALDI probe. The figure represents the spectra obtained in negative and positive ion mode, respectively. Analyte concentration: 200 $\mu\text{g}/\text{mL}$. Humic acid (HA) is widely distributed in nature and is known for its strong affinity for heavy metals and organic pollutants present in the environment.¹⁶ This property makes it a significant representative substance of environmental interference factors. We found that the presence of HA did not interfere with the process of enrichment and screening of Py-Azo-COF as a SALDI probe when toxic chemicals were tested individually. All twelve toxic compounds were successfully detected with clear distinction. This observation highlights the potential applicability of this method in environmental samples.

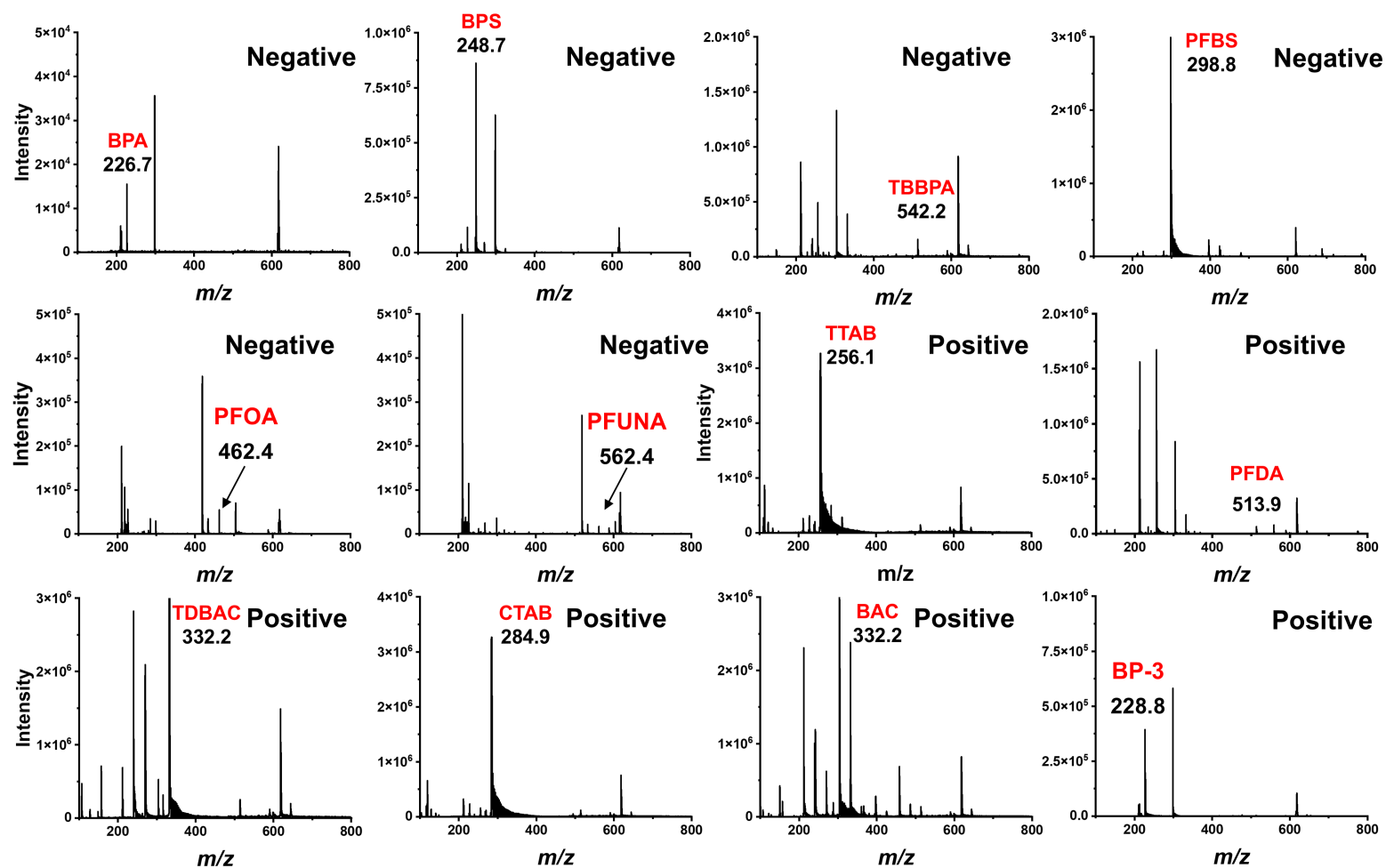


Fig. S17. Effect of salinity (*i.e.*, NaCl) on MS performance of Py-Azo-COF as a SALDI probe. The figure represents the spectra obtained in negative and positive ion mode, respectively. Analyte concentration: 200 $\mu\text{g/mL}$. In the presence of NaCl, all twelve toxic compounds were successfully detected individually, meeting the standard requirements without any interference. This result shows the effectiveness of this method in accurately identifying toxic chemicals within a high salinity environment.

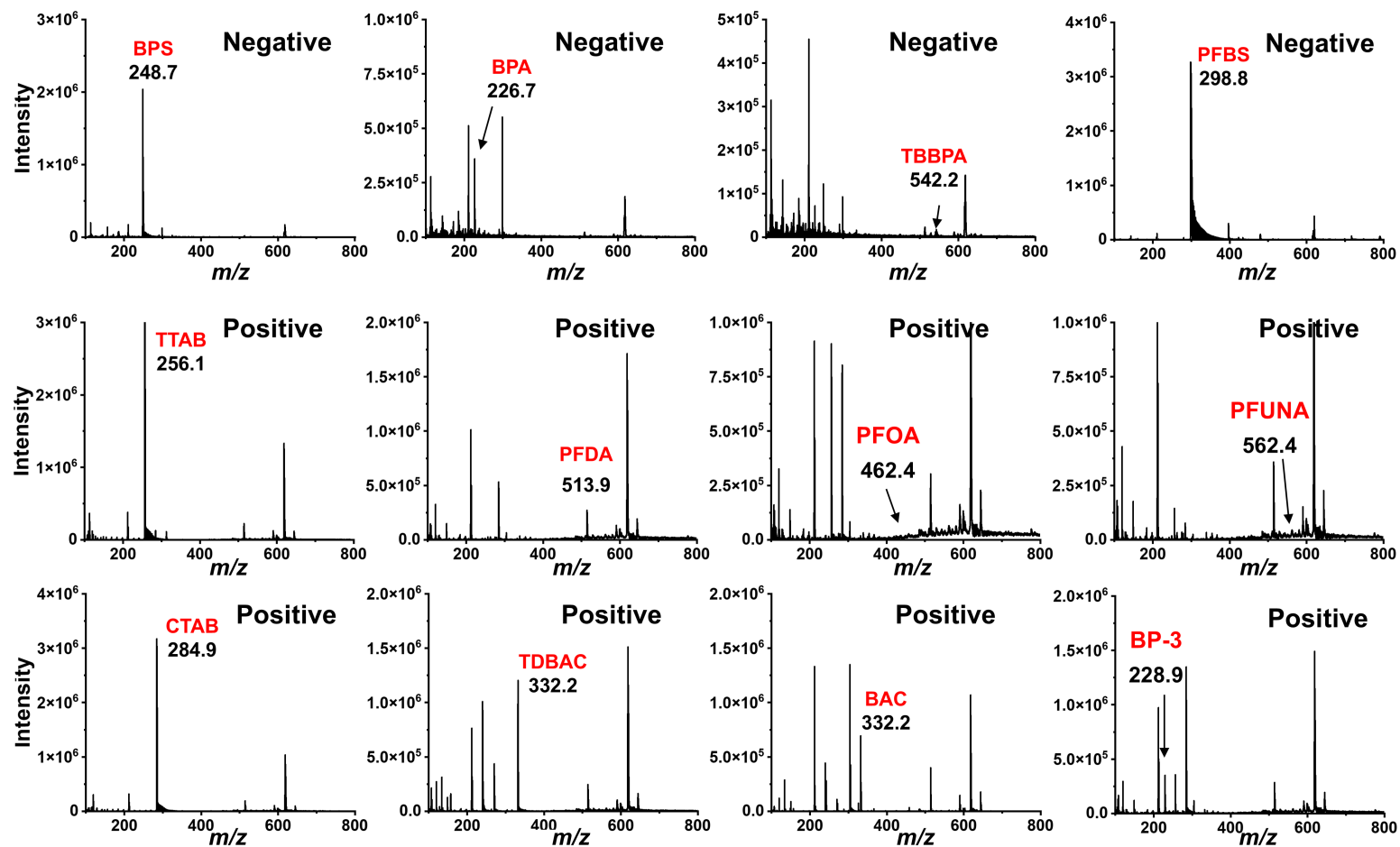


Fig. S18. Effect of biological factor (*i.e.*, BSA) on MS performance of Py-Azo-COF as a SALDI probe. The figure represents the spectra obtained in negative and positive ion mode, respectively. Analyte concentration: 200 $\mu\text{g}/\text{mL}$. The presence of biological factors (BSA) did not interfere with the individual screening of twelve typical toxic compounds by Py-Azo-COF. This finding confirms the capability of method to effectively detect target compounds in biological samples. The application of Py-Azo-COF in biological samples holds significant practical value due to the potential entry of trace toxic compounds into organisms through the food chains in the environment.

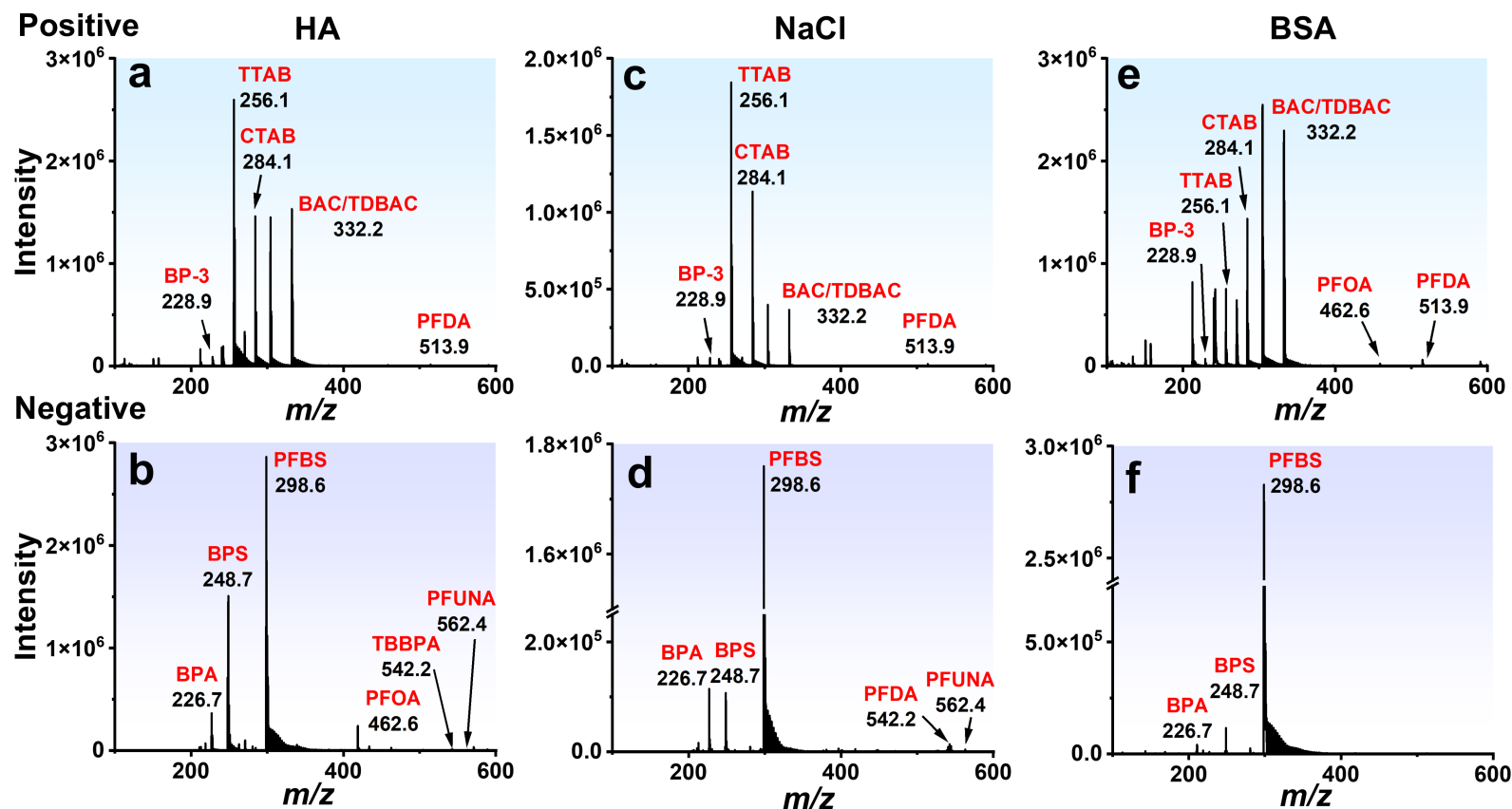


Fig. S19. Mass spectra of toxic chemicals with Py-Azo-COF as a SALDI probe in the presence of HA, BSA, and NaCl by dual-ion-mode LDI-TOF MS.

The top (a, c, e) and bottom (b, d, f) represent the spectra obtained in positive and negative ion mode, respectively. Analyte concentration: 33 $\mu\text{g/mL}$. The interfering substances include HA(a), NaCl(c), and BSA(e). Py-Azo-COF exhibits significant potential for applications in environmental and biological samples, as well as in high-salt environments. It effectively enables the enrichment and screening of a wide range of toxic compounds in a mixture, without any notable background interference. Particularly noteworthy is the outstanding performance of Py-Azo-COF when applied to environmental samples, making it highly suitable for the simultaneous screening of multiple pollutants in real environmental scenarios.

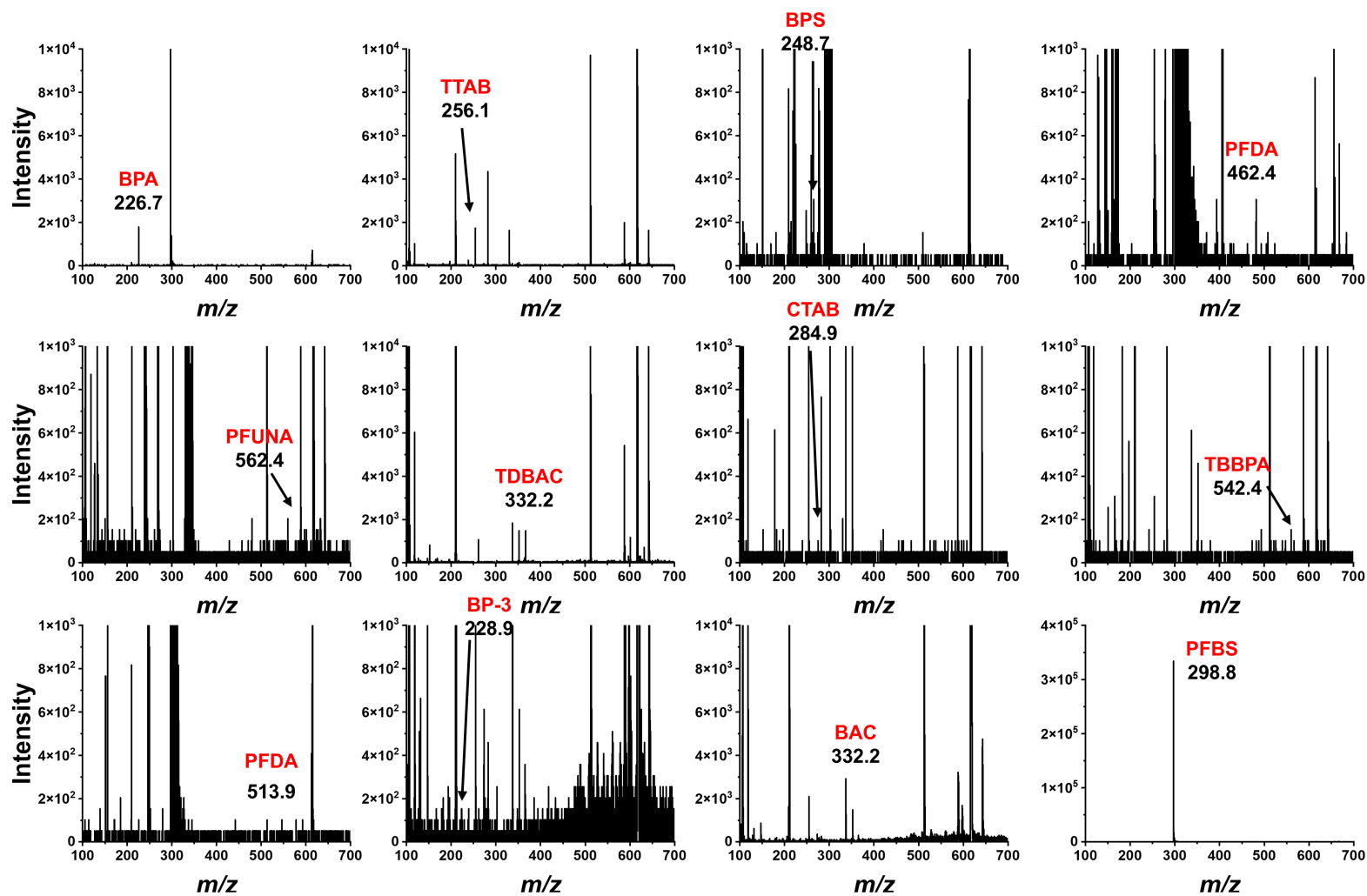


Fig. S20. The mass spectra of toxic chemicals at LOD using Py-Azo-COF as a SALDI probe by dual-ion mode LDI-TOF MS. The LOD was determined by diluting the standard samples with the lowest concentration within the dynamic linear range. The LOD was defined as the minimum concentration value from three parallel samples that could generate a reliable measurement signal (S/N ratio > 3).

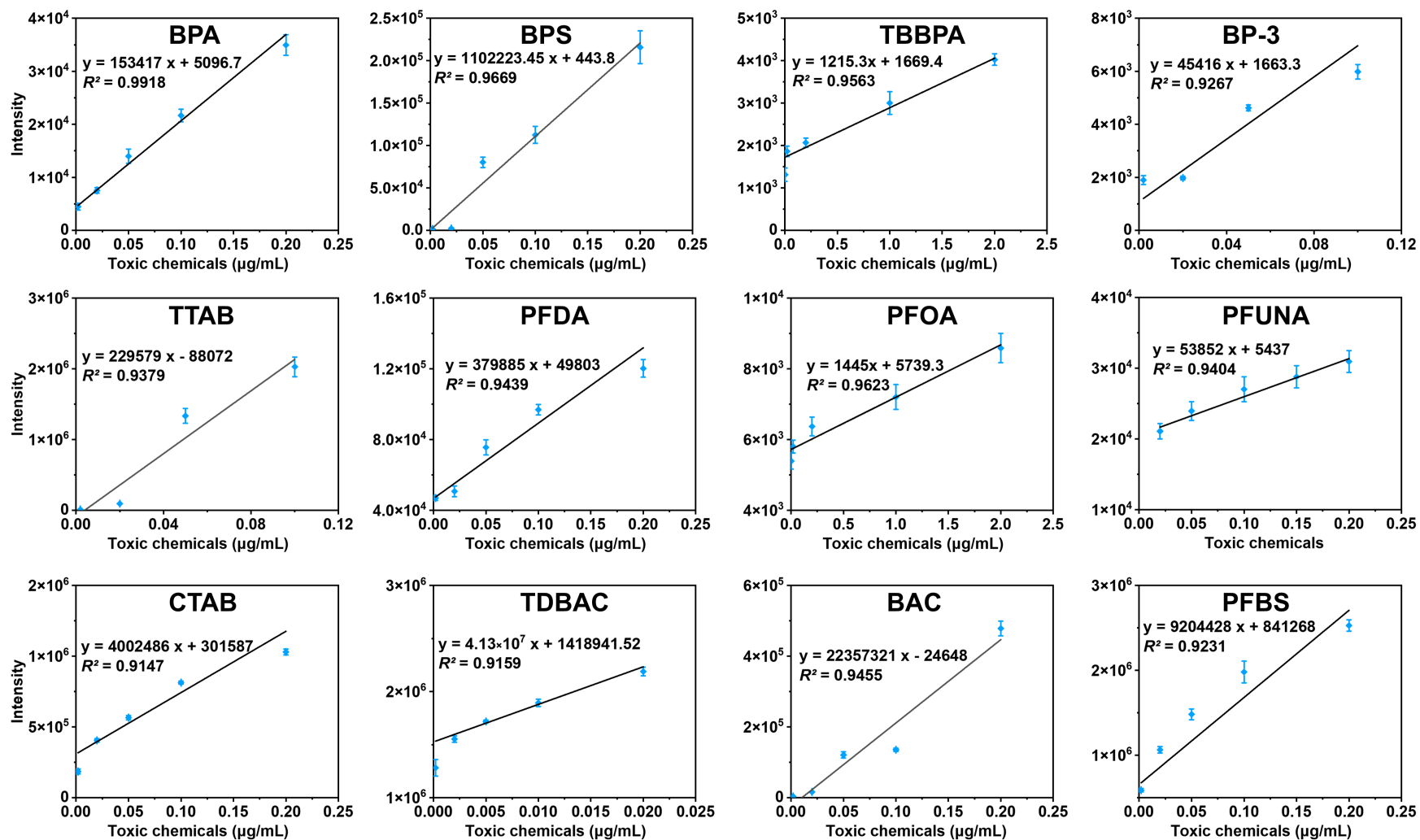


Fig. S21. The standard curve of toxic chemicals using Py-Azo-COF as a SALDI probe by dual-ion mode LDI-TOF MS. Error bars indicate the standard deviation from three independent experiments.

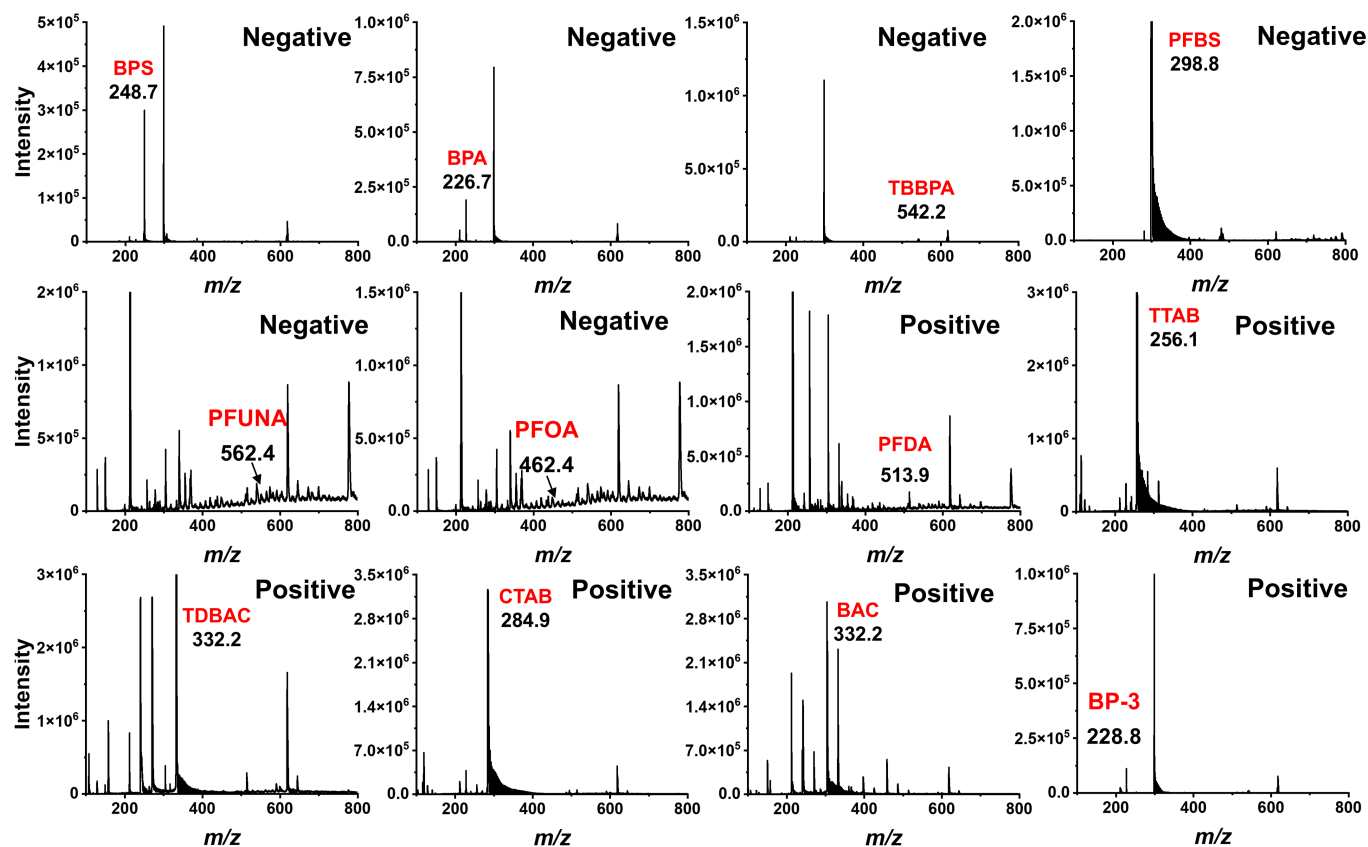


Fig. S22. Screening of different types of toxic chemicals in spiked wastewater sample by using Py-Azo-COF as a SALDI probe. The figure represents the spectra obtained in negative and positive ion mode, respectively. Analyte concentration: 200 $\mu\text{g/mL}$. The wastewater from the electronics factory contains significant amounts of heavy metals and organic pollutants, which potentially pose challenges to the accurate detection of the target analytes. However, in the presence of trace amounts of toxic chemicals added to samples taken from the wastewater, Py-Azo-COF showed its ability to detect twelve specific toxic compounds. This observation indicates that Py-Azo-COF possesses certain anti-interference capabilities and can selectively enrich samples during actual detection processes.

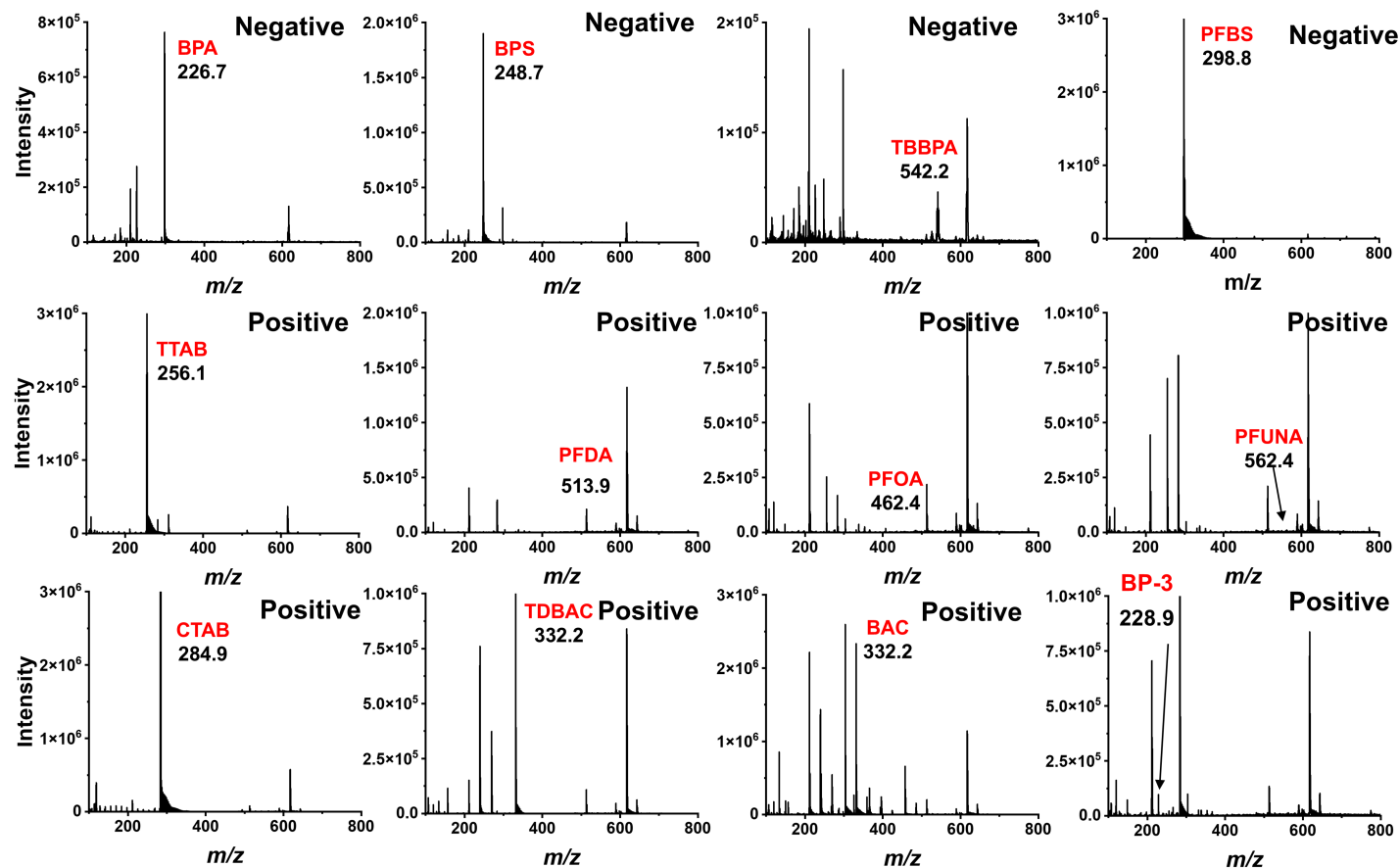


Fig. S23. Screening of different types of toxic chemicals in spiked sewage sludge sample by using Py-Azo-COF as a SALDI probe. The figure represents the spectra obtained in negative and positive ion mode, respectively. Analyte concentration: 200 $\mu\text{g/mL}$. Twelve toxic compound standards were added to the leachate solution of sewage sludge obtained from the electronics plant. Despite the existence of various organic substances in the soil leachate, which led to the appearance of peaks from other compounds in the mass spectra, the accurate detection of the target compounds by Py-Azo-COF was not compromised.

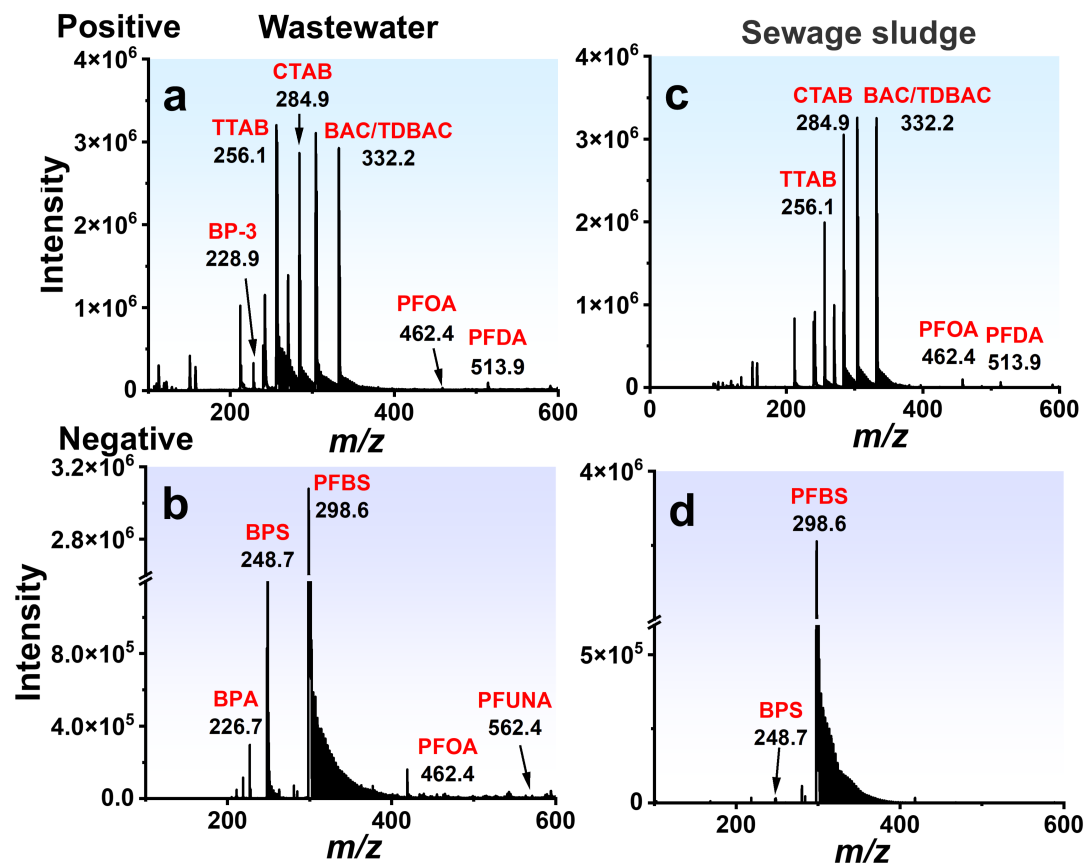


Fig. S24. Mass spectra of toxic chemicals with Py-Azo-COF as a SALDI probe in spiked wastewater and sewage sludge samples. The top (a, c) and bottom (b, d) represent the spectra obtained in positive and negative ion mode, respectively. Analyte concentration: 33 $\mu\text{g}/\text{mL}$. A mixture of twelve toxic compounds was added to the wastewater and sewage sludge leachate obtained from the electronics factories. In the wastewater, a total of eleven toxic chemicals were detected, while the sewage sludge leachate contained eight toxic compounds. The complexity of the composition in actual samples may give rise to interference effects among different substances, resulting in reduced screening efficiency. However, Py-Azo-COF indicated notable advantages compared to other methods, as it enabled screening of multiple toxic compounds rather than just a single one.

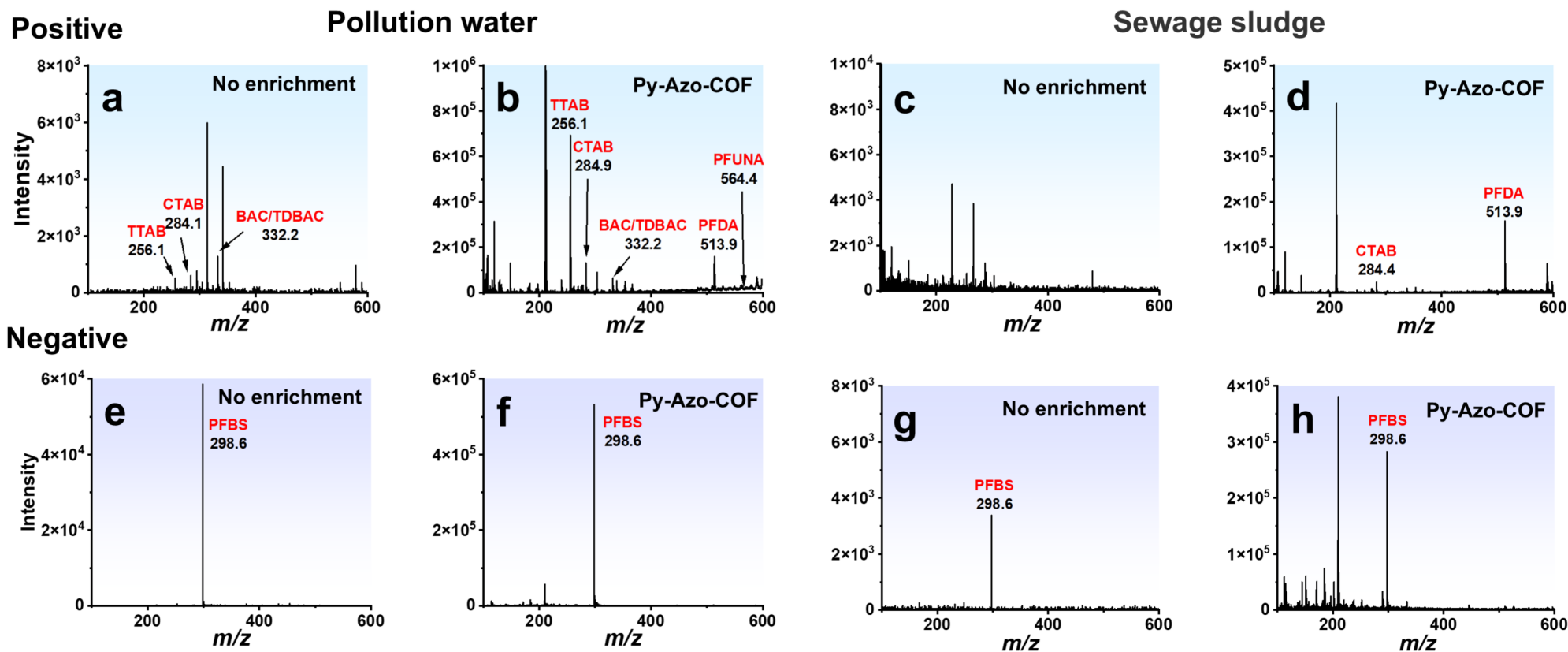


Fig. S25. Identification and screening of different types of toxic chemicals in real wastewater and sewage sludge samples collected from twelve municipal electronic factories. (a-d) Real wastewater samples and (e-h) sewage sludge samples. The top (a-d) and bottom (e-h) represent the spectra obtained in positive and negative ion mode, respectively. When Py-Azo-COF was not used as a probe, PFBS, TDBAC, TTAB, and CTAB were detected in the wastewater samples, and only PFBS was detected in the sewage sludge. Following the introduction of Py-Azo-COF as an SALDI probe into real samples, a significant increase in the peak intensity of trace-level toxic chemicals was observed and contaminants such as PFDA and PFUNA could be identified.

REFERENCE

- 1 Q. Liu, M. Cheng, J. Wang and G. Jiang, *Chem. – Eur. J.*, 2015, **21**, 5594–5599.
- 2 X. Huang, Q. Liu, X. Huang, Z. Nie, T. Ruan, Y. Du and G. Jiang, *Anal. Chem.*, 2017, **89**, 1307–1314.
- 3 X. Huang, Q. Liu and G. Jiang, *Talanta*, 2019, **199**, 532–540.
- 4 C. Li, H. Geng, X. Zhu, C. Gao, N. Jiang, Y. Qiao and Q. Cai, *Microchem. J.*, 2020, **152**, 104294.
- 5 K. Luo, B. Yang, W. Guo, Q. Sun, O. Dan, Z. Lin and Z. Cai, *Analyst*, 2020, **145**, 5664–5669.
- 6 H. Chen, D. Qi, C. Deng, P. Yang and X. Zhang, *Proteomics*, 2009, **9**, 380–387.
- 7 Q. Sun, C. Gao, W. Ma, Y. He, J. Wu, K. Lou, D. Ouyang, Z. Lin and Z. Cai, *Microchim. Acta*, **2020**, 187,370.
- 8 E. Al-Hetlani, M. O. Amin, M. Madkour and A. A. Nazeer, *Talanta*, 2018, **185**, 439–445.
- 9 K. H. Langford and K. V. J. Thomas, *Environ. Monit*, 2008, **10**, 894–898.
- 10 J. Nelson, F. Bishay, A. van Roodselaar, M. Ikonomou and F. C. P. Law, *Sci. Total Environ*, 2007, **374**, 80–90.
- 11 A. Speltini, M. Maiocchi, L. Cucca, D. Merli and A. Profumo, *Anal. Bioanal. Chem*, 2014, **406**, 3657–3665.
- 12 J. Magnér, M. Filipovic and T. Alsberg, *Chemosphere*, 2010, **80**, 1255–1260.
- 13 L. Ye, J. Liu, X. Yang, Y. Peng, L. Xu, *J. Sep. Sci*, 2011, **34**, 700-706.
- 14 N. S. Lisboa, C. S. Fahning, G. Cotrim, J. P. dos Anjos, J. B. de Andrade, V. Hatje, G. O. da Rocha, *Talanta*, 2013, **117**, 168-175.
- 15 J. T. Althakafy, C. Kulsing, M. R. Grace and P. J. Marriott, *J. Sep. Sci*, 2018, **41**, 3706-3715.
- 16 S. Chianese, A. Fenti, P. Iovino, D. Musmarra and S. Salvestrini, *Molecules*, 2020, **25**, 918.